SIAM J. NUMER. ANAL.
Vol. 60, No. 1, pp. 52–75
© 2022 Society for Industrial and Applied Mathematics

Downloaded 05/04/22 to 144.174.212.73 . Redistribution subject to SIAM license or copyright; see https://epubs.siam.org/terms-privacy

LOCKING-FREE ENRICHED GALERKIN METHOD FOR LINEAR ELASTICITY*

SON-YOUNG YI†, SANGHYUN LEE‡, AND LUDMIL ZIKATANOV§

Abstract. We propose a new locking-free enriched Galerkin method for solving the linear elasticity problem. The method is based on the discontinuous Galerkin formulation, but its approximation space is a continuous piecewise linear vector-valued function space enriched by some discontinuous piecewise linear functions. An a priori error estimate of optimal order in the energy norm is proved and shown to be independent of a Lamé parameter λ, hence the proposed method is free of volumetric locking when modeling incompressible materials. Moreover, a uniform preconditioner with respect to the mesh size is established in the operator preconditioning framework. We provide several numerical examples to confirm the accuracy and the robustness of the new method and demonstrate a good performance of the preconditioner.

Key words. linear elasticity, enriched Galerkin method, locking-free, operator preconditioning

AMS subject classifications. 65N30, 65N55, 65F08, 74S05

DOI. 10.1137/21M1391353

1. Introduction.

Let Ω be a bounded, connected, Lipschitz domain in $\mathbb{R}^d$, $d = 2, 3$, with boundary $\partial\Omega$. Then, the governing equation for linear elasticity reads as follows: Find the displacement $u \in \mathbb{R}^d$ that satisfies

$$-\nabla \cdot \boldsymbol{\sigma}(u) = f \quad \text{in } \Omega, \tag{1.1a}$$

$$u = u_D \quad \text{on } \partial\Omega, \tag{1.1b}$$

where f is an external body force. Here, $\boldsymbol{\sigma}$ is the symmetric $d \times d$ stress tensor defined as

$$\boldsymbol{\sigma}(u) := 2\mu\boldsymbol{\epsilon}(u) + \lambda(\nabla \cdot u)\mathbf{I},$$

where $\boldsymbol{\epsilon}(u) = \frac{1}{2}(\nabla u + (\nabla u)^T)$ is the strain tensor, $\mathbf{I}$ is the $d \times d$ identity tensor, and λ and μ are the Lamé parameters such that $0 < \lambda < \infty$ and $0 < \mu_1 < \mu < \mu_2$ for some positive constants μ_1 and μ_2. In the case of plane strain, λ and μ can be rewritten as

$$\lambda = \frac{E\nu}{(1+\nu)(1-2\nu)} \quad \text{and} \quad \mu = \frac{E}{2(1+\nu)},$$

where E is the modulus of elasticity, and ν is Poisson's ratio. In this paper, we will assume that $f \in L^2(\Omega)^d$ and $u_D = \widetilde{u_D}|_{\partial\Omega}$ for some $\widetilde{u_D} \in H^2(\Omega)^d$ and that the true solution u satisfies the following H^2-regularity:

$$\|u\|_2 + \lambda\|\nabla \cdot u\|_1 \le C(\|f\|_0 + \|\widetilde{u_D}\|_2), \tag{1.2}$$

*Received by the editors January 14, 2021; accepted for publication (in revised form) September 14, 2021; published electronically January 5, 2022.
https://doi.org/10.1137/21M1391353
Funding: The work of the second author was partially supported by National Science Foundation (NSF) grant DMS-1913016.
†Department of Mathematical Sciences, University of Texas at El Paso, El Paso, TX 79968 USA (syi@utep.edu).
‡Department of Mathematics, Florida State University, Tallahassee, FL 32306 USA (lee@math.fsu.edu).
§Department of Mathematics, Pennsylvania State University, University Park, PA 16802 USA (ludmil02@gmail.com).

Copyright © by SIAM. Unauthorized reproduction of this article is prohibited.

Downloaded 05/04/22 to 144.174.212.73 . Redistribution subject to SIAM license or copyright; see https://epubs.siam.org/terms-privacy

where $C > 0$ is independent of the Lamé constant λ. The other notation including the Sobolev norms will be defined in section 2. The regularity assumption (1.2) is true if Ω is sufficiently smooth or if Ω is a convex polygon in two dimensions [41, 10]. In three-dimensional cases, it is very technical to derive such regularity. See the monograph [20] for details.

As the Lamé constant λ tends to ∞ (equivalently, when $\nu \to 1/2$), the material becomes nearly incompressible. The incompressibility of the material can be described mathematically by $\nabla \cdot u \approx 0$, which can be derived from (1.2) as $\lambda \to \infty$. It is well known that this incompressibility constraint may cause a loss of uniformity (with respect to λ) in the convergence regime of a low-order continuous Galerkin (CG) method, a phenomenon known as volumetric locking.

There exists an extensive literature that proposed alternative numerical methods to alleviate locking in linear elasticity. The most popular methods fall into classes of mixed finite element methods [5, 4, 47, 48, 6], nonconforming finite element methods [16, 10], and discontinuous Galerkin (DG) methods [34, 42, 43], among others. Mixed finite element methods tend to be locking-free and provide accurate stress approximations; however, the choice of mixed finite element spaces is restricted due to the well-known inf-sup condition. On the other hand, DG methods employ function spaces that are only piecewise continuous, and thus often comprise more inclusive function spaces than traditional CG methods. Moreover, they allow the possibility of high-order methods on unstructured mesh while maintaining high locality. Nevertheless, DG methods have some disadvantages in efficiency due to the large number of degrees of freedom, which in turn requires an efficient linear solver. In order to address such disadvantages of the DG methods, more efficient variants of DG methods, including the hybridizable DG methods [38, 17] and embedded DG methods [14], have been proposed.

In this paper, we propose an enriched Galerkin (EG) method for solving the linear elasticity problem. The original EG method, which we refer to as the locally conservative EG (LC-EG) method, was introduced by Sun and Liu [39] for solving a second-order elliptic problem and was tested for a coupled flow and transport problem in porous media. The crux of their idea was to enrich the approximation space of the classical CG method with piecewise constant functions and use it in the DG formulation. Thus, one can achieve the local mass conservation property inherited from the DG method at a low computational cost comparable to that of the CG method. Since then, the LC-EG method has been successfully employed to problems of modeling flow and transport in porous media [28, 29, 30, 35, 27, 3], the shallow water equations [23], computational poromechanics [12, 18, 25, 26], and the Stokes equations [11].

The main goal of this paper is to propose and analyze a locking-free EG (LF-EG) method. Indeed, there was a prior attempt by Mital [33] to utilize the LC-EG method for solving the linear elasticity problem with a moderate-sized λ. As a matter of fact, the LC-EG space is still not rich enough to approximate the divergence-free state of the solution when λ is very large. In light of this observation, we propose to enrich the linear CG space with some discontinuous piecewise linear vector-valued functions whose gradient is a constant multiple of the identity tensor in each element. Indeed, this new enriched function space requires only one additional local degree of freedom (DoF) in each element compared to the linear CG space. Therefore, it requires even fewer DoFs than the linear LC-EG space and significantly fewer DoFs than the linear DG space. Yet, the new space now has nontrivial divergence-free functions, hence the potential for the locking-free property. To distinguish this new

Copyright © by SIAM. Unauthorized reproduction of this article is prohibited.

Downloaded 05/04/22 to 144.174.212.73 . Redistribution subject to SIAM license or copyright; see https://epubs.siam.org/terms-privacy

EG method from the LC-EG method, we will refer to the new EG method as the LF-EG method. Besides the aforementioned advantages, one can utilize the existing CG and DG codes to implement the LF-EG method with some slight modifications. Among recent work related to ours is work by Harper et al. [22] in that they also use enriched Lagrangian finite elements but on quadrilateral and hexahedral meshes. However, their enrichment spaces consist of edge/face-based bubble vector functions, hence requiring more DoFs than our method. Moreover, their weak formulation is based on the reduced integration method, unlike our DG-type weak formulation.

In this paper, we prove existence and uniqueness of the solution for our LF-EG method and establish an optimal-order error estimate in the energy norm in which the error bound is independent of λ. Therefore, our LF-EG method is locking-free even for a large λ. To construct a uniform preconditioner (with respect to the mesh size), we utilize the operator-preconditioning framework developed by [31] and [32]. In that framework, constructing field-of-values equivalent preconditioners amounts to the construction of an operator that provides a norm that is equivalent to the energy norm. Our choice for such construction is the well-known additive Schwarz preconditioner (see, e.g., [40, 44, 19, 45]) corresponding to an appropriate splitting of the underlying finite element space.

We provide several numerical experiments in two dimensions to support our theoretical results of the optimal convergence rate and the locking-free property of the LF-EG method. For each example, we solve the problem using both our LF-EG method and the classical linear CG method for the sake of comparison and demonstrate the advantage of our new method over the linear CG method when simulating incompressible materials. We also include some results of numerical experiments illustrating the performance of the proposed additive Schwarz preconditioner.

The rest of this paper is organized as follows. In section 2, some useful notation and preliminaries are introduced. Then, the new LF-EG method for the linear elasticity problem is introduced in section 3 and a convergence analysis is presented in section 4. Then, in section 5, we propose a preconditioner for the linear system resulting from the LF-EG method. Finally, some numerical results are provided in section 6.

2. Notation and preliminaries. In this section, we will introduce some notation and preliminaries that will be useful throughout the rest of the paper. We use the standard notation for Sobolev spaces [1] and their norms. For example, let $E \subset \mathbb{R}^d$ be a bounded domain; then the space $H^s(E)$ for integer s is

$$H^s(E) = \{v \in L^2(E) \ : \ \forall 0 \le |\omega| \le s,\, D^\omega v \in L^2(E)\},$$

where the vector space $L^2(E)$ is the space of square-integrable functions, and for a multi-index $\omega = (\omega_1, \ldots, \omega_d) \in \mathbb{N}^d$ such that $|\omega| = \sum_{i=1}^d \omega_i$, $D^\omega v$ is the distributional derivative. The Sobolev norm and seminorm associated with $H^s(E)$ are denoted by $\|\cdot\|_{s,E}$ and $|\cdot|_{s,E}$, respectively. We extend these definitions and notation naturally to vector functions $\zeta : E \to \mathbb{R}^d$ and tensor functions $\boldsymbol{\tau} : E \to \mathbb{R}^{d\times d}$. When $s = 0$, $H^s(E)$ coincides with $L^2(E)$, and the inner product will be denoted by $(\cdot,\cdot)_E$ in this case. For simplicity, the subscript E will be dropped if $E = \Omega$.

On the other hand, broken Sobolev spaces are natural spaces to work with the DG and EG methods, and these spaces depend on the partition of the domain. Let $\mathcal{T}_h$ be the shape-regular triangulation by a family of partitions of Ω into elements T, where T is a triangle when $d = 2$ or a tetrahedron when $d = 3$. We denote by h_T the diameter of T, and we set $h = \max_{T\in\mathcal{T}_h} h_T$. Let n_T be the unit outward normal

Copyright © by SIAM. Unauthorized reproduction of this article is prohibited.

Downloaded 05/04/22 to 144.174.212.73 . Redistribution subject to SIAM license or copyright; see https://epubs.siam.org/terms-privacy

vector to ∂T for $T \in \mathcal{T}_h$. The broken Sobolev space $H^s(\mathcal{T}_h)$ for any real number s is defined by

$$H^s(\mathcal{T}_h) = \{v \in L^2(\Omega) : v|_T \in H^s(T) \ \ \forall T \in \mathcal{T}_h\}.$$

Again, these definitions and notation can be naturally extended to vector and tensor functions.

In addition, we denote by $\mathcal{E}_h$ the set of all edges (or faces) and by $\mathcal{E}_h^I$ and $\mathcal{E}_h^\partial$ the collections of all interior and boundary edges (faces), respectively. For any $e \in \mathcal{E}_h^I$, there are two neighboring elements T^+ and T^- such that $e = \partial T^+ \cap \partial T^-$. We associate one unit normal vector n_e with e, which is assumed to be oriented from T^+ to T^-. If $e \in \mathcal{E}_h^\partial$, then n_e is taken to be the unit outward normal vector to $\partial\Omega$.

Now, we define the jump and average of functions in $H^1(\mathcal{T}_h)^d$ on $e \in \mathcal{E}_h$. For $\zeta \in H^1(\mathcal{T}_h)^d$, the trace of ζ along ∂T for any element T is well defined. If $e \in \mathcal{E}_h^I$ is shared by two elements T^+ and T^-, there are two traces of ζ on e, which will be denoted by $\zeta^\pm$, respectively. Now, we introduce the so-called average operator $\{\cdot\}$ on $e \in \mathcal{E}_h^I$ as follows:

$$\{\zeta\} := \frac{1}{2}\left(\zeta^+ + \zeta^-\right).$$

Also, the jump across interior edges $e \in \mathcal{E}_h^I$ will be defined by

$$[\![\zeta]\!] := \zeta^+ - \zeta^-.$$

On the other hand, on the boundary edges $e \in \mathcal{E}_h^\partial$, we set

$$\{\zeta\} = [\![\zeta]\!] := \zeta.$$

We close this section by recalling some important trace inequalities that will frequently be used in the analysis of our EG method. Let $|T|$ denote the area of T in two dimensions and the volume of T in three dimensions. Similarly, for $e \subset \partial T$, $|e|$ denotes the length of e in two dimensions and the area of e in three dimensions. Then, there is a constant C_t independent of h_T and v such that for any $v \in H^s(T)$, $s \geq 1$,

$$\|v\|_{0,e} \leq C_t h_T^{-1/2}(\|v\|_{0,T} + h_T\|\nabla v\|_{0,T}) \quad \forall e \subset \partial T. \tag{2.1}$$

Let $\mathbb{P}_k(T)$ be the space of polynomials of total degree at most k for a nonnegative integer k. If $v \in \mathbb{P}_k(T)$, then the trace inequality becomes

$$\|v\|_{0,e} \leq \tilde{C}_t h_T^{-1/2}\|v\|_{0,T} \quad \forall e \subset \partial T, \tag{2.2}$$

where $\tilde{C}_t$ is independent of h_T and v but depends on the polynomial degree k. Analogous results to (2.1) and (2.2) still hold for vector- and tensor-valued functions.

3. Locking-free enriched Galerkin method for linear elasticity. In this section, we will define our LF-EG method and prove its solvability. First, let us introduce the finite element space. Let $\mathcal{M}_h$ be the standard finite element space of d-vectors whose components are continuous piecewise linear polynomials:

$$\mathcal{M}_h := \left\{\psi \in H^1(\Omega)^d |\ \psi|_T \in \mathbb{P}_1(T)^d \ \forall T \in \mathcal{T}_h\right\}. \tag{3.1}$$

Also, let

$$\mathcal{D}_h := \left\{\psi \in L^2(\Omega)^d |\ \psi|_T = c_T(\mathbf{x} - \mathbf{x}_T),\ c_T \in \mathbb{R},\ \forall T \in \mathcal{T}_h\right\},$$

Copyright © by SIAM. Unauthorized reproduction of this article is prohibited.

where $\mathbf{x} = [x_1, \ldots, x_d]^t$ and $\mathbf{x}_T$ is the position vector of the center of $T \in \mathcal{T}_h$, that is, $(\mathbf{x} - \mathbf{x}_T, 1)_T = 0$. We note that $\mathcal{M}_h$ and $\mathcal{D}_h$ are disjoint subspaces of the linear DG space

$$\left\{\psi \in L^2(\Omega)^d |\ \psi|_T \in \mathbb{P}_1(T)^d\ \forall T \in \mathcal{T}_h\right\}.$$

Then, the LF-EG finite element space $\mathcal{V}_h$ is defined as a direct sum of these two spaces:

$$\mathcal{V}_h := \mathcal{M}_h \oplus \mathcal{D}_h.$$

It is worth mentioning that we deliberately chose the space $\mathcal{D}_h$ instead of the piecewise constant vector-valued space used in the existing LC-EG method [33]. Recall that the linear CG space $\mathcal{M}_h$ suffers from locking because it is not rich enough to have nontrivial divergence-free vectors.

The LF-EG space requires only N_T more DoFs compared to that of the linear CG (P_1-CG) space method regardless of the dimension d, where N_T is the number of elements T in $\mathcal{T}_h$. This means that the LF-EG method requires fewer DoFs than the LC-EG method and significantly fewer DoFs than the linear DG (P_1-DG) method. Figure 1 illustrates the DoFs on a coarse two-dimensional Cartesian grid for four compatible methods employing piecewise linear vector-valued polynomials: P_1-CG, P_1-DG, LC-EG, and our new LF-EG methods.

Now, we are in a position to present the LF-EG method. Our LF-EG method for solving the linear elasticity problem (1.1) reads as follows: Find $U \in \mathcal{V}_h$ such that

$$\mathcal{S}(U, v) = \mathcal{F}(v) \quad \forall\, v \in \mathcal{V}_h, \tag{3.2}$$

where $\mathcal{S}$ and $\mathcal{F}$ are the bilinear form and linear functional, respectively, defined as

$$\begin{aligned}
\mathcal{S}(U,v) :=& \sum_{T\in\mathcal{T}_h} (\boldsymbol{\sigma}(U), \boldsymbol{\epsilon}(v))_T - \sum_{e\in\mathcal{E}_h} (\{\boldsymbol{\sigma}(U)n_e\}, [\![v]\!])_e \\
&+ \sum_{e\in\mathcal{E}_h} ([\![U]\!], \{\boldsymbol{\sigma}(v)n_e\})_e + \sum_{e\in\mathcal{E}_h} \frac{\alpha}{h_e} ([\![U]\!], [\![v]\!])_e, + \lambda^2 \sum_{e\in\mathcal{E}_h^I} \beta h_e ([\![\nabla\cdot U]\!], [\![\nabla\cdot v]\!])_e, \\
\mathcal{F}(v) :=& \sum_{T\in\mathcal{T}_h} (f, v)_T + \sum_{e\in\mathcal{E}_h^\partial} (u_D, \boldsymbol{\sigma}(v)n_e)_e + \sum_{e\in\mathcal{E}_h^\partial} \frac{\alpha}{h_e} (u_D, v)_e,
\end{aligned}$$

where $\alpha > 0$ and $\beta > 0$ are penalty parameters, and h_e is defined by $h_e = |e|^{\frac{1}{d-1}}$. In general, the penalty parameters may vary over e, but we assume that they are constants in this paper. Also, notice that the Dirichlet boundary condition (1.1b) is

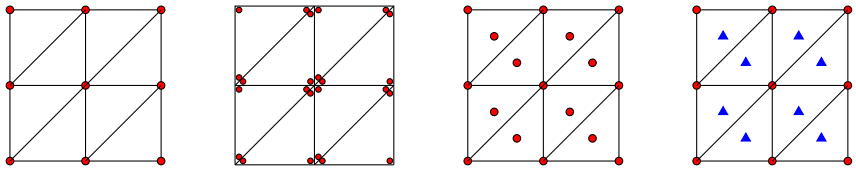

(a) P_1-CG. (b) P_1-DG. (c) LC-EG. (d) LF-EG.

FIG. 1. *Comparison of DoFs on a two-dimensional Cartesian grid for four methods:* (a) P_1-*CG,* (b) P_1-*DG ,* (c) *LC-EG, and* (d) *LF-EG methods. A red circle (●) represents two DoFs and a blue triangle (▲) represents one DoF.*

Downloaded 05/04/22 to 144.174.212.73 . Redistribution subject to SIAM license or copyright; see https://epubs.siam.org/terms-privacy

Copyright © by SIAM. Unauthorized reproduction of this article is prohibited.

Downloaded 05/04/22 to 144.174.212.73 . Redistribution subject to SIAM license or copyright; see https://epubs.siam.org/terms-privacy

imposed weakly in this method. The following generalized Korn's inequality easily follows from (1.19) in [8]: There is a constant $C_{Korn} > 0$ such that

$$\sum_{T\in\mathcal{T}_h} \|\nabla v\|_{0,T}^2 \le C_{Korn}\left(\sum_{T\in\mathcal{T}_h} \|\boldsymbol{\epsilon}(v)\|_{0,T}^2 + \sum_{e\in\mathcal{E}_h} \frac{1}{h_e}\| [\![v]\!] \|_{0,e}^2\right) \quad \forall v \in \mathcal{V}_h. \tag{3.3}$$

In light of the above Korn's inequality, we now introduce the following energy norm for $\alpha > 0$ in the LF-EG finite element space $\mathcal{V}_h$:

$$\|v\|_{\mathcal{E}} = \left(\sum_{T\in\mathcal{T}_h} \|\boldsymbol{\epsilon}(v)\|_{0,T}^2 + \sum_{e\in\mathcal{E}_h} \frac{\alpha}{h_e}\| [\![v]\!] \|_{0,e}^2\right).$$

3.1. Consistency.

LEMMA 3.1. *Let u be the solution of* (1.1) *and assume that $u \in H^s(\Omega)^d$ for $s > 3/2$. Then, u satisfies the variational problem* (3.2)*:*

$$\mathcal{S}(u, v) = \mathcal{F}(v) \quad \forall v \in \mathcal{V}_h. \tag{3.4}$$

Proof. Multiply (1.1a) by $v \in \mathcal{V}_h$ on both sides, then integrate using Green's theorem and the symmetry of the stress tensor:

$$\begin{aligned} -\sum_{T\in\mathcal{T}_h} (\nabla\cdot\boldsymbol{\sigma}(u), v)_T &= \sum_{T\in\mathcal{T}_h} (\boldsymbol{\sigma}(u), \boldsymbol{\epsilon}(v))_T - \sum_{T\in\mathcal{T}_h} (\boldsymbol{\sigma}(u)n_T, v)_{\partial T} \\ &= \sum_{T\in\mathcal{T}_h} (\boldsymbol{\sigma}(u), \boldsymbol{\epsilon}(v))_T - \sum_{e\in\mathcal{E}_h} (\{\boldsymbol{\sigma}(u)n_e\}, [\![v]\!])_e - \sum_{e\in\mathcal{E}_h^I} ([\![\boldsymbol{\sigma}(u)n_e]\!], \{v\})_e \\ &= \sum_{T\in\mathcal{T}_h} (\boldsymbol{\sigma}(u), \boldsymbol{\epsilon}(v))_T - \sum_{e\in\mathcal{E}_h} (\{\boldsymbol{\sigma}(u)n_e\}, [\![v]\!])_e, \end{aligned} \tag{3.5}$$

where the continuity of the normal stress $\boldsymbol{\sigma}(u)n_e$ across the interior edges was used in the last equality. Also, the jump $[\![u]\!] = 0$ and $[\![\nabla\cdot u]\!] = 0$ across all the interior edges due to the regularity of u, hence

$$\sum_{e\in\mathcal{E}_h^I} ([\![u]\!], \{\boldsymbol{\sigma}(v)n_e\})_e = 0, \quad \sum_{e\in\mathcal{E}_h^I} \frac{\alpha}{h_e}([\![u]\!], [\![v]\!])_e = 0, \quad \lambda^2 \sum_{e\in\mathcal{E}_h^I} \beta h_e([\![\nabla\cdot u]\!], [\![\nabla\cdot v]\!])_e = 0.$$

Adding these three terms on the far right-hand side of (3.5), we have

$$\begin{aligned} &\sum_{T\in\mathcal{T}_h} (\boldsymbol{\sigma}(u), \boldsymbol{\epsilon}(v))_T - \sum_{e\in\mathcal{E}_h} (\{\boldsymbol{\sigma}(u)n_e\}, [\![v]\!])_e + \sum_{e\in\mathcal{E}_h^I} ([\![u]\!], \{\boldsymbol{\sigma}(v)n_e\})_e \\ &\quad + \sum_{e\in\mathcal{E}_h^I} \frac{\alpha}{h_e}([\![u]\!], [\![v]\!])_e + \lambda^2 \sum_{e\in\mathcal{E}_h^I} \beta h_e([\![\nabla\cdot u]\!], [\![\nabla\cdot v]\!])_e = \sum_{T\in\mathcal{T}_h} (f, v)_T. \end{aligned} \tag{3.6}$$

On the other hand, using the boundary condition (1.1b), we have

$$\sum_{e\in\mathcal{E}_h^\partial} ([\![u]\!], \{\boldsymbol{\sigma}(v)n_e\})_e + \sum_{e\in\mathcal{E}_h^\partial} \frac{\alpha}{h_e}([\![u]\!], [\![v]\!])_e = \sum_{e\in\mathcal{E}_h^\partial} (u_D, \boldsymbol{\sigma}(v)n_e)_e + \sum_{e\in\mathcal{E}_h^\partial} \frac{\alpha}{h_e}(u_D, v)_e. \tag{3.7}$$

Then, we add (3.7) to (3.6) and obtain $\mathcal{S}(u, v) = \mathcal{F}(v)$. ∎

Copyright © by SIAM. Unauthorized reproduction of this article is prohibited.

Downloaded 05/04/22 to 144.174.212.73 . Redistribution subject to SIAM license or copyright; see https://epubs.siam.org/terms-privacy

3.2. Coercivity.

LEMMA 3.2. *There exists a positive constant C_{coer} independent of h and λ such that*

$$\mathcal{S}(v,v) \geq C_{coer}\|v\|_{\mathcal{E}}^2 + \lambda^2 \sum_{e\in\mathcal{E}_h^I} \beta h_e \| [\![\nabla\cdot v]\!] \|_{0,e}^2 \quad \forall v \in \mathcal{V}_h \tag{3.8}$$

for any penalty parameters $\alpha > 0$ and $\beta > 0$.

Proof. It is straightforward to see that

$$\begin{aligned}\mathcal{S}(v,v) = 2\mu \sum_{T\in\mathcal{T}_h} \|\boldsymbol{\epsilon}(v)\|_{0,T}^2 + \lambda \sum_{T\in\mathcal{T}_h} \|\nabla\cdot v\|_{0,T}^2 + \sum_{e\in\mathcal{E}_h} \frac{\alpha}{h_e} \| [\![v]\!] \|_{0,e}^2 \\ + \lambda^2 \sum_{e\in\mathcal{E}_h^I} \beta h_e \| [\![\nabla\cdot v]\!] \|_{0,e}^2 \geq \min(2\mu,1)\|v\|_{\mathcal{E}}^2 + \lambda^2 \sum_{e\in\mathcal{E}_h^I} \beta h_e \| [\![\nabla\cdot v]\!] \|_{0,e}^2.\end{aligned}$$

Therefore, (3.8) holds with $C_{coer} = \min(2\mu, 1)$. ∎

3.3. Solvability.

LEMMA 3.3. *There exists a unique solution U to problem* (3.2).

Proof. Due to the finite-dimensionality, it suffices to prove uniqueness. Let U_1 and U_2 be two solutions to the LF-EG scheme (3.2). Then, we have

$$\mathcal{S}(U_1 - U_2, v) = 0 \quad \forall v \in \mathcal{V}_h.$$

Taking $v = U_1 - U_2$ and using (3.8), we have $\|U_1 - U_2\|_{\mathcal{E}} = 0$, hence $U_1 = U_2$. ∎

4. Convergence analysis.

4.1. Interpolation operator. For the convergence analysis, we need to define an interpolation operator from $H^1(\Omega)^d$ to $\mathcal{V}_h$. As we want to prove an error estimate that is independent of the Lamé constant λ, the interpolation operator should be able to preserve the divergence-free vector at least in a weak sense. To this end, let $\Pi_h^c : H^1(\Omega)^d \to \mathcal{M}_h$ be a Clément-type interpolant satisfying

$$|v - \Pi_h^c v|_{j,T} \leq C h_T^{m-j} |v|_{m,\Delta_T}, \quad 0 \leq j \leq m \leq 2, \ \forall v \in H^2(\Omega)^d, \forall T \in \mathcal{T}_h, \tag{4.1}$$

where C is independent of h and T, and Δ_T is a macroelement containing T used for defining $\Pi_h^c v$. Then, we define $\Pi_h^d : H^1(\Omega)^d \to \mathcal{D}_h$ such that

$$(\nabla\cdot\Pi_h^d v, 1)_T = (\nabla\cdot(v - \Pi_h^c v), 1)_T \quad \forall T \in \mathcal{T}_h.$$

Owing to the fact $\nabla\cdot\Pi_h^d v|_T \in \mathbb{P}_0(T)$, it is easy to see that

$$\nabla\cdot\Pi_h^d v|_T = \frac{1}{|T|}(\nabla\cdot(v - \Pi_h^c v), 1)_T \stackrel{def}{=} c_T \quad \forall T \in \mathcal{T}_h,$$

from which we can express $\Pi_h^d v|_T$ explicitly as

$$\Pi_h^d v|_T = \frac{c_T}{d}(\mathbf{x} - \mathbf{x}_T). \tag{4.2}$$

Finally, we define $\Pi_h : H^1(\Omega)^d \to \mathcal{V}_h$ by

$$\Pi_h := \Pi_h^c + \Pi_h^d.$$

Copyright © by SIAM. Unauthorized reproduction of this article is prohibited.

Downloaded 05/04/22 to 144.174.212.73 . Redistribution subject to SIAM license or copyright; see https://epubs.siam.org/terms-privacy

LEMMA 4.1. *We have the following interpolation error estimates for* Π_h*:*

$$|\nabla \cdot (v - \Pi_h v)|_j \le C h^{1-j} |\nabla \cdot v|_1, \quad 0 \le j \le 1, \quad \forall v \in H^2(\Omega)^d, \tag{4.3a}$$

$$|v - \Pi_h v|_j \le C h^{m-j} |v|_m, \qquad 0 \le j \le m \le 2, \quad \forall v \in H^2(\Omega)^d. \tag{4.3b}$$

Proof. It is straightforward to see that

$$(\nabla \cdot (v - \Pi_h v), 1)_T = (\nabla \cdot v - \nabla \cdot \Pi_h v, 1)_T = 0 \quad \forall T \in \mathcal{T}_h, \tag{4.4}$$

which implies that

$$\mathcal{P}_0(\nabla \cdot v) = \nabla \cdot (\Pi_h v) \ \text{ on each } T \in \mathcal{T}_h, \tag{4.5}$$

where $\mathcal{P}_0$ is the local L^2-projection onto the piecewise-constant space on $\mathcal{T}_h$. Therefore,

$$|\nabla \cdot (v - \Pi_h v)|_{j,T} = |\nabla \cdot v - \mathcal{P}_0(\nabla \cdot v)|_{j,T} \le C h_T^{1-j} |\nabla \cdot v|_{1,T}, \ j = 0, 1.$$

After summing the square of both sides over $T \in \mathcal{T}_h$ and taking the square root, we obtain the desired error estimate (4.3a). To prove (4.3b), we first note that the result is trivial when $j = m = 2$ since $\Pi_h v|_T \in \mathbb{P}_1(T)^d$. In the case of $j = 0, 1$, it suffices to show that

$$|\Pi_h^d v|_j \le C h^{m-j} |v|_m, \quad j \le m \le 2, \tag{4.6}$$

thanks to the triangle inequality and (4.1). To this end, we will first provide the bound for $|\Pi_h^d v|_0$, i.e., $j = 0$. Using (4.2), the Cauchy–Schwarz inequality, and (4.1), we have

$$\begin{aligned}
\sum_{T \in \mathcal{T}_h} |\Pi_h^d v|_{0,T}^2 &= \sum_{T \in \mathcal{T}_h} \frac{c_T^2}{d^2} \int_T (\mathbf{x} - \mathbf{x}_T)^2 \, d\mathbf{x} \\
&= \sum_{T \in \mathcal{T}_h} \frac{1}{d^2} \left(\frac{1}{|T|} \int_T \nabla \cdot (v - \Pi_h^c v) \, dx \right)^2 \int_T (\mathbf{x} - \mathbf{x}_T)^2 \, d\mathbf{x} \\
&\le \sum_{T \in \mathcal{T}_h} \frac{1}{d^2 |T|} \|\nabla \cdot (v - \Pi_h^c v)\|_{0,T}^2 \|\mathbf{x} - \mathbf{x}_T\|_{\infty,T}^2 |T| \\
&\le \sum_{T \in \mathcal{T}_h} \frac{1}{d^2} \|\nabla \cdot (v - \Pi_h^c v)\|_{0,T}^2 h_T^2 \le \sum_{T \in \mathcal{T}_h} \frac{h_T^2}{d^2} |v - \Pi_h^c v|_{1,T}^2 \\
&\le C \sum_{T \in \mathcal{T}_h} h_T^{2m} |v|_{m,\Delta_T}^2 \le C h^{2m} |v|_m, \quad m = 1, 2.
\end{aligned}$$

It remains to prove (4.6) with $j = 1$ and it can be done similarly by noting from (4.2) that

$$|\Pi_h^d v|_{1,T}^2 = \frac{1}{d} c_T^2 |T|. \qquad \square$$

4.2. Energy-norm error estimate. In this section, we will prove an a priori error estimate for the approximate solution in the energy norm. First, let $\eta = u - \Pi_h u$ and $\xi = \Pi_h u - U$, then, $u - U = \eta + \xi$. We will start with the following lemma that will be useful for our error analysis.

Copyright © by SIAM. Unauthorized reproduction of this article is prohibited.

LEMMA 4.2. *There exists a constant $C > 0$ independent of h and λ such that*

$$|\boldsymbol{\sigma}(\eta)|_j \le Ch^{1-j}(\|f\|_0 + \|\widetilde{u_D}\|_2), \quad j = 0, 1. \tag{4.7}$$

Proof. Using the interpolation errors (4.3a) and (4.3b), we obtain

$$\begin{aligned} |\boldsymbol{\sigma}(\eta)|_j = |2\mu\boldsymbol{\epsilon}(\eta) + \lambda(\nabla\cdot\eta)\mathbf{I}|_j &\le C(|\eta|_{j+1} + \lambda|\nabla\cdot\eta|_j) \\ &\le Ch^{1-j}(|u|_2 + \lambda|\nabla\cdot u|_1), \quad j = 0, 1. \end{aligned}$$

The desired result follows from the regularity of the solution (1.2). ∎

LEMMA 4.3. *We have the following error estimate for the auxiliary variable $\xi = \Pi_h u - U$:*

$$\|\xi\|_{\mathcal{E}} \le Ch(\|f\|_0 + \|\widetilde{u_D}\|_2),$$

where $C > 0$ depends on μ but is independent of h and λ.

Proof. First, we obtain the following consistency equation by subtracting (3.2) from (3.4),

$$\mathcal{S}(u - U, v) = 0 \quad \forall v \in \mathcal{V}_h, \tag{4.8}$$

from which we have $\mathcal{S}(\eta + \xi, \xi) = 0$ since $\xi \in \mathcal{V}_h$. Hence, $\mathcal{S}(\xi, \xi) = -\mathcal{S}(\eta, \xi)$. On the other hand, $(\nabla\cdot\eta, \nabla\cdot\xi)_T = 0$ on each T since $\nabla\cdot\xi \in \mathbb{P}_0(T)$. Therefore, we have

$$\begin{aligned} \mathcal{S}(\xi,\xi) &= -2\mu\sum_{T\in\mathcal{T}_h}(\boldsymbol{\epsilon}(\eta),\boldsymbol{\epsilon}(\xi))_T + \sum_{e\in\mathcal{E}_h}(\{\boldsymbol{\sigma}(\eta)n_e\},[\![\xi]\!])_e - \sum_{e\in\mathcal{E}_h}([\![\eta]\!],\{\boldsymbol{\sigma}(\xi)n_e\})_e \\ &\quad - \sum_{e\in\mathcal{E}_h}\frac{\alpha}{h_e}([\![\eta]\!],[\![\xi]\!])_e - \lambda^2\sum_{e\in\mathcal{E}_h^I}\beta h_e([\![\nabla\cdot\eta]\!],[\![\nabla\cdot v]\!])_e \\ &:= \Phi_1 + \Phi_2 + \Phi_3 + \Phi_4 + \Phi_5. \end{aligned}$$

First, we will consider $\mathcal{S}(\xi, \xi)$ on the left-hand side. Using the coercivity result (3.8), we immediately have

$$C_{coer}\|\xi\|_{\mathcal{E}}^2 + \lambda^2\sum_{e\in\mathcal{E}_h^I}\beta h_e\|\,[\![\nabla\cdot\xi]\!]\,\|_{0,e}^2 \le \sum_{i=1}^{5}|\Phi_i|. \tag{4.9}$$

We will bound each $|\Phi_i|$, $i = 1, \ldots, 5$, using primarily the Cauchy–Schwarz and Young's inequalities, trace inequalities, and interpolation error bounds. First, for a small $\delta_1 > 0$, we get

$$\begin{aligned} |\Phi_1| &\le 2\mu\sum_{T\in\mathcal{T}_h}|(\boldsymbol{\epsilon}(\eta),\boldsymbol{\epsilon}(\xi))_T| \le 2\mu\left(\sum_{T\in\mathcal{T}_h}\|\boldsymbol{\epsilon}(\eta)\|_{0,T}^2\right)^{\frac{1}{2}}\left(\sum_{T\in\mathcal{T}_h}\|\boldsymbol{\epsilon}(\xi)\|_{0,T}^2\right)^{\frac{1}{2}} \\ &\le \delta_1\|\boldsymbol{\epsilon}(\xi)\|_0^2 + C\|\boldsymbol{\epsilon}(\eta)\|_0^2 \le \delta_1\|\xi\|_{\mathcal{E}}^2 + Ch^2\|u\|_2^2. \end{aligned}$$

Next, we bound $|\Phi_2|$ using the trace inequality (2.1) and (4.7) as follows:

$$\begin{aligned} |\Phi_2| &\le \sum_{e\in\mathcal{E}_h}|(\{\boldsymbol{\sigma}(\eta)n_e\},[\![\xi]\!])_e| \le \left(\sum_{e\in\mathcal{E}_h}\frac{h_e}{\alpha}\|\,\{\boldsymbol{\sigma}(\eta)n_e\}\,\|_{0,e}^2\right)^{\frac{1}{2}}\left(\sum_{e\in\mathcal{E}_h}\frac{\alpha}{h_e}\|\,[\![\xi]\!]\,\|_{0,e}^2\right)^{\frac{1}{2}} \\ &\le \delta_2\|\xi\|_{\mathcal{E}}^2 + C\sum_{T\in\mathcal{T}_h}(\|\sigma(\eta)\|_{0,T} + h_T|\sigma(\eta)|_{1,T})^2 \\ &\le \delta_2\|\xi\|_{\mathcal{E}}^2 + Ch^2(\|u\|_2 + \lambda\|\nabla\cdot u\|_1)^2 \end{aligned}$$

for a small constant $\delta_2 > 0$.

Copyright © by SIAM. Unauthorized reproduction of this article is prohibited.

Downloaded 05/04/22 to 144.174.212.73 . Redistribution subject to SIAM license or copyright; see https://epubs.siam.org/terms-privacy

Downloaded 05/04/22 to 144.174.212.73 . Redistribution subject to SIAM license or copyright; see https://epubs.siam.org/terms-privacy

Let us now turn our attention to the next term $|\Phi_3|$. First, we recall that $(\nabla\cdot\eta,\nabla\cdot\xi)_T=0$ on each $T\in\mathcal{T}_h$. Therefore,

$$0=\sum_{T\in\mathcal{T}_h}(\nabla\cdot\eta,\nabla\cdot\xi)_T=\sum_{T\in\mathcal{T}_h}(\eta\cdot n_T,\nabla\cdot\xi)_{\partial T}=\sum_{e\in\mathcal{E}_h}(\llbracket\eta\cdot n_e\rrbracket,\{\nabla\cdot\xi\})_e + \sum_{e\in\mathcal{E}_h^I}(\{\eta\cdot n_e\},\llbracket\nabla\cdot\xi\rrbracket)_e.$$

Then,

$$\begin{aligned}|\Phi_3|&=\left|\sum_{e\in\mathcal{E}_h}(\llbracket\eta\rrbracket,\{\boldsymbol{\sigma}(\xi)n_e\})_e\right|=\left|2\mu\sum_{e\in\mathcal{E}_h}(\llbracket\eta\rrbracket,\{\boldsymbol{\epsilon}(\xi)n_e\})_e+\lambda\sum_{e\in\mathcal{E}_h}(\llbracket\eta\cdot n_e\rrbracket,\{\nabla\cdot\xi\})_e\right|\\&=\left|2\mu\sum_{e\in\mathcal{E}_h}(\llbracket\eta\rrbracket,\{\boldsymbol{\epsilon}(\xi)n_e\})_e-\lambda\sum_{e\in\mathcal{E}_h^I}(\{\eta\cdot n_e\},\llbracket\nabla\cdot\xi\rrbracket)_e\right|\\&\le 2\mu\sum_{e\in\mathcal{E}_h}\|\llbracket\eta\rrbracket\|_{0,e}\|\{\boldsymbol{\epsilon}(\xi)n_e\}\|_{0,e}+\lambda\sum_{e\in\mathcal{E}_h^I}\|\{\eta\cdot n_e\}\|_{0,e}\|\llbracket\nabla\cdot\xi\rrbracket\|_{0,e}\\&\le\delta_3\sum_{T\in\mathcal{T}_h}\|\boldsymbol{\epsilon}(\xi)\|_{0,T}^2+\frac{\lambda^2}{4}\sum_{e\in\mathcal{E}_h^I}\beta h_e\|\llbracket\nabla\cdot\xi\rrbracket\|_{0,e}^2+C\sum_{T\in\mathcal{T}_h}\frac{1}{h_T^2}(\|\eta\|_{0,T}+h_T|\eta|_{1,T})^2\\&\le\delta_3\sum_{T\in\mathcal{T}_h}\|\xi\|_{\mathcal{E}}^2+\frac{\lambda^2}{4}\sum_{e\in\mathcal{E}_h^I}\beta h_e\|\llbracket\nabla\cdot\xi\rrbracket\|_{0,e}^2+Ch^2\|u\|_2^2,\end{aligned}$$

where $\delta_3>0$ is a small constant and $C>0$ depends on μ and the constants C_t and $\tilde{C}_t$ from the trace inequalities.

The fourth term $|\Phi_4|$ can be bounded in a similar fashion:

$$\begin{aligned}|\Phi_4|&\le\sum_{e\in\mathcal{E}_h}\left|\frac{\alpha}{h_e}(\llbracket\eta\rrbracket,\llbracket\xi\rrbracket)_e\right|\le\left(\sum_{e\in\mathcal{E}_h}\frac{\alpha}{h_e}\|\llbracket\eta\rrbracket\|_{0,e}^2\right)^{\frac12}\left(\sum_{e\in\mathcal{E}_h}\frac{\alpha}{h_e}\|\llbracket\xi\rrbracket\|_{0,e}^2\right)^{\frac12}\\&\le\delta_4\|\xi\|_{\mathcal{E}}^2+C\sum_{T\in\mathcal{T}_h}\frac{\alpha}{h_T^2}(\|\eta\|_{0,T}^2+h_T^2|\eta|_{1,T}^2)\le\delta_4\|\xi\|_{\mathcal{E}}^2+Ch^2\|u\|_2^2\end{aligned}$$

for a small constant $\delta_4>0$.

Let us now consider the last term $|\Phi_5|$.

$$\begin{aligned}|\Phi_5|&\le\lambda^2\sum_{e\in\mathcal{E}_h^I}|\beta h_e(\llbracket\nabla\cdot\eta\rrbracket,\llbracket\nabla\cdot\xi\rrbracket)_e|\le\lambda^2\left(\sum_{e\in\mathcal{E}_h^I}\beta h_e\|\llbracket\nabla\cdot\eta\rrbracket\|_{0,e}^2\right)^{\frac12}\left(\sum_{e\in\mathcal{E}_h^I}\beta h_e\|\llbracket\nabla\cdot\xi\rrbracket\|_{0,e}^2\right)^{\frac12}\\&\le\frac{\lambda^2}{4}\sum_{e\in\mathcal{E}_h^I}\beta h_e\|\llbracket\nabla\cdot\xi\rrbracket\|_{0,e}^2+C\beta\lambda^2\sum_{T\in\mathcal{T}_h}(\|\nabla\cdot\eta\|_{0,T}+h_T\|\nabla\cdot\eta\|_{1,T})^2\\&\le\frac{\lambda^2}{4}\sum_{e\in\mathcal{E}_h^I}\beta h_e\|\llbracket\nabla\cdot\xi\rrbracket\|_{0,e}^2+Ch^2\lambda^2\|\nabla\cdot u\|_1^2.\end{aligned}$$

Combining the above bounds for $|\Phi_i|, i=1,\dots,5$, with (4.9) and using the H^2-regularity (1.2), we have

$$\begin{aligned}(C_{coer}-\sum_{i=1}^4\delta_i)\|\xi\|_{\mathcal{E}}^2+\frac{\lambda^2}{2}\sum_{e\in\mathcal{E}_h^I}\beta h_e\|\llbracket\nabla\cdot\xi\rrbracket\|_{0,e}^2&\le Ch^2(\|u\|_2^2+\lambda^2\|\nabla\cdot u\|_1^2)\\&\le Ch^2(\|f\|_0+\|\widetilde{u_D}\|_2)^2,\end{aligned}$$

Copyright © by SIAM. Unauthorized reproduction of this article is prohibited.

where $C = C(\mu, C_t, \tilde{C}_t, \alpha, \frac{1}{\alpha}, \beta, \frac{1}{\beta})$ is independent of h and λ. Recall that C_{coer} is also independent of h and λ. By taking sufficiently small $\delta_i's$, we can make the coefficient $(C_{coer} - \sum_{i=1}^4 \delta_i)$ positive on the left-hand side. Then, we arrive at

$$\left(C_{coer} - \sum_{i=1}^{4} \delta_i\right) \|\xi\|_{\mathcal{E}}^2 \leq Ch^2(\|f\|_0 + \|\widetilde{u_D}\|_2)^2.$$

Finally, we divide both sides by $(C_{coer} - \sum_{i=1}^4 \delta_i)$ to complete the proof. ∎

Now, we are ready to present the main error estimate.

THEOREM 4.4. *Let u be the solution of the elasticity problem* (1.1) *and U be the solution of our LF-EG method* (3.2)*. Assuming the H^2-regularity of the solution in* (1.2)*, there is a constant $C > 0$ such that*

$$\|u - U\|_{\mathcal{E}} \leq Ch(\|f\|_0 + \|\widetilde{u_D}\|_2),$$

where C is independent of h and λ.

Proof. The result is a consequence of the error estimate for ξ in Lemma 4.3, the interpolation error estimate (4.3b), and the triangle inequality. ∎

5. Preconditioning. We propose a uniform preconditioner with respect to the mesh size for our LF-EG method when λ is bounded. The construction of the preconditioner is done using the operator preconditioning framework [31, 32].

Consider the operator $S : \mathcal{V}_h \to \mathcal{V}_h'$ defined via $\mathcal{S}(\cdot, \cdot)$:

$$(Sv, w) := \mathcal{S}(v, w) \quad \forall v, w \in \mathcal{V}_h. \tag{5.1}$$

We also introduce a bilinear form $a(\cdot, \cdot)$ which generates the energy norm:

$$a(v, w) := a_C(v, w) + a_J(v, w) \quad \forall v, w \in \mathcal{V}_h, \tag{5.2}$$

where

$$a_C(v, w) := \sum_{T \in \mathcal{T}_h} (\boldsymbol{\epsilon}(v), \boldsymbol{\epsilon}(w))_T \quad \text{and} \quad a_J(v, w) := \sum_{e \in \mathcal{E}_h} \frac{\alpha_e}{h_e} (\llbracket v \rrbracket, \llbracket w \rrbracket)_e. \tag{5.3}$$

By the definition of $a(\cdot, \cdot)$ we have that $a(v, v) = \|v\|_{\mathcal{E}}^2$.

We say that two symmetric bilinear forms $a(\cdot, \cdot)$ and $b(\cdot, \cdot)$ are spectrally equivalent, which is denoted by $b(\cdot, \cdot) \eqsim a(\cdot, \cdot)$, if and only if there exist positive constants c_0 and c_1 such that

$$c_0 b(v, v) \leq a(v, v) \leq c_1 b(v, v). \tag{5.4}$$

As $a(\cdot, \cdot)$ defines the energy inner product and norm, any spectrally equivalent bilinear form $b(\cdot, \cdot)$ defines an inner product on $\mathcal{V}_h$ and a corresponding norm $\|\cdot\|_b$. The Riesz operator $A : \mathcal{V}_h \to \mathcal{V}_h'$ associated with $a(\cdot, \cdot)$ is defined as

$$(Av, w) = a(v, w) \quad \forall v, w \in \mathcal{V}_h. \tag{5.5}$$

We will use a bilinear form $b(\cdot, \cdot)$ to define a preconditioner $B \approx A^{-1}$, which is an approximate inverse of A. Following this convention, we denote the Riesz operator corresponding to $b(\cdot, \cdot)$ by $B^{-1} : \mathcal{V}_h \to \mathcal{V}_h'$ whose definition is

$$(B^{-1}v, w) = b(v, w) \quad \forall v, w \in \mathcal{V}_h. \tag{5.6}$$

Copyright © by SIAM. Unauthorized reproduction of this article is prohibited.

Downloaded 05/04/22 to 144.174.212.73 . Redistribution subject to SIAM license or copyright; see https://epubs.siam.org/terms-privacy

Downloaded 05/04/22 to 144.174.212.73 . Redistribution subject to SIAM license or copyright; see https://epubs.siam.org/terms-privacy

In our presentations, $(\cdot,\cdot)$ may denote the duality pairing $\mathcal{V}_h' \times \mathcal{V}_h \to \mathbb{R}$, or it may be another inner product which is a realization of the duality pairing, e.g., the $L^2(\Omega)$-inner product. The particular form of the pairing does not affect the considerations that follow. We also note the following relation:

$$(B^{-1}v, v) = (A(BA)^{-1}v, v) = a((BA)^{-1}v, v). \tag{5.7}$$

The use of an inverse operator will be justified when we show later that $b(\cdot,\cdot)$ is spectrally equivalent to $a(\cdot,\cdot)$, which is coercive on $\mathcal{V}_h$ and induces the energy norm.

To show that our preconditioner is uniform with respect to the mesh size, we will utilize the continuity of $\mathcal{S}$: There exists a constant $\gamma > 0$ such that

$$\sup_{v\in\mathcal{V}_h}\sup_{w\in\mathcal{V}_h}\frac{\mathcal{S}(v,w)}{\|w\|_{\mathcal{E}}\|v\|_{\mathcal{E}}} \le \gamma. \tag{5.8}$$

The existence of such a constant γ when the Lamé parameter λ is bounded above can be proved using the trace inequality and the inequality $\|\nabla\cdot v\|_0 \le \sqrt{d}\|\boldsymbol{\epsilon}(v)\|_0$. Next, recall that we have already shown the coercivity of $\mathcal{S}(\cdot,\cdot)$ on $\mathcal{V}_h$ in Lemma 3.2. This implies the following inf-sup condition:

$$\inf_{v\in\mathcal{V}_h}\sup_{w\in\mathcal{V}_h}\frac{\mathcal{S}(v,w)}{\|w\|_{\mathcal{E}}\|v\|_{\mathcal{E}}} \ge C_{\mathrm{coer}} > 0. \tag{5.9}$$

We note that the inequalities (5.8) and (5.9) still hold if the energy norm $\|\cdot\|_{\mathcal{E}}$ is replaced with its equivalent norm. Based on this observation, we will use a bilinear form $b(\cdot,\cdot)$ that is spectrally equivalent to $a(\cdot,\cdot)$, thus whose induced norm $\|\cdot\|_b$ is equivalent to $\|\cdot\|_{\mathcal{E}}$, to construct a preconditioner.

5.1. Field-of-values equivalent preconditioner. Our LF-EG method results in a nonsymmetric linear system. Following [31], we utilize field-of-values equivalent preconditioners to obtain an efficient linear solver.

Definition 5.1 (field-of-values equivalent preconditioner). *The operators B and S are* field-of-values equivalent *if there are positive constants c_{lo} and c_{up} such that for any $v \in \mathcal{V}_h$ there holds*

$$c_{lo} \le \frac{b(BSv, v)}{b(v, v)} \quad \textit{and} \quad \frac{\sqrt{b(BSv, BSv)}}{\sqrt{b(v, v)}} \le c_{up}. \tag{5.10}$$

Indeed, we can show the field-of-values equivalence of B and S if $b(\cdot,\cdot) \eqsim a(\cdot,\cdot)$.

Lemma 5.2. *Assume that $b(\cdot,\cdot)$ and $a(\cdot,\cdot)$ are spectrally equivalent, namely, there exist constants c_0 and c_1 such that* (5.4) *holds. Then B and S are field-of-values equivalent.*

Proof. To prove the first inequality in (5.10), we use (5.6), (5.4), and (5.9) to see

$$\frac{b(BSv, v)}{c_0 b(v, v)} = \frac{(Sv, v)}{c_0 b(v, v)} \ge \frac{(Sv, v)}{a(v, v)} = \frac{(Sv, v)}{\|v\|_{\mathcal{E}}^2} \ge C_{\mathrm{coer}},$$

which implies the first inequality with $c_{\mathrm{lo}} = c_0 C_{\mathrm{coer}}$. The second inequality can be shown in a similar fashion using (5.4), (5.6), and (5.8),

$$\frac{\sqrt{b(BSv, BSv)}}{\sqrt{b(v, v)}} = \frac{1}{\|v\|_b}\sup_{w\in\mathcal{V}_h}\frac{b(BSv, w)}{\|w\|_b} = \frac{1}{\|v\|_b}\sup_{w\in\mathcal{V}_h}\frac{(Sv, w)}{\|w\|_b} \le c_1 \sup_{w\in\mathcal{V}_h}\frac{(Sv, w)}{\|v\|_{\mathcal{E}}\|w\|_{\mathcal{E}}} \le c_1\gamma,$$

which shows the second inequality with $c_{\mathrm{up}} = c_1\gamma$. ∎

Copyright © by SIAM. Unauthorized reproduction of this article is prohibited.

Downloaded 05/04/22 to 144.174.212.73 . Redistribution subject to SIAM license or copyright; see https://epubs.siam.org/terms-privacy

We now provide a result on the convergence of the field-of-values preconditioned GMRES [37, 36] method as stated and proved in [31, Theorem 2.8].

THEOREM 5.3 (convergence of preconditioned GMRES). *Assume that $b(\cdot,\cdot)$ and $a(\cdot,\cdot)$ are spectrally equivalent. If v^m is the mth iteration of the GMRES method, and U is the exact solution of $SU = F$, then*

$$\frac{\|BS(U-v^m)\|_{\mathcal{E}}}{\|BS(U-v^0)\|_{\mathcal{E}}} \leq \left(1-\frac{c_{lo}^2}{c_{up}^2}\right)^{m/2}. \tag{5.11}$$

Based on this theorem, we will construct a preconditioner that will result in a uniformly bounded contraction in every GMRES iteration. In light of Lemma 5.2 and Theorem 5.3, it only remains for us to construct a bilinear form $b(\cdot,\cdot)$ that is spectrally equivalent to $a(\cdot,\cdot)$ and whose variational problem is easier to solve.

5.2. Construction of $b(\cdot,\cdot)$. In order to define a preconditioning bilinear form $b(\cdot,\cdot)$, we will employ the standard additive Schwarz preconditioner and show the spectral equivalence (5.4). The theoretical results that we present here is considered classical and is found in [40, 44, 45, 19] and other references cited therein. To keep the presentation self-contained, we provide some details below even though most of them are available in the aforementioned works. We will explore the idea that the space complementary to $\mathcal{M}_h$ contains highly oscillatory functions whose energy norm behaves like an appropriately scaled L^2-norm.

5.2.1. Notation and preliminaries. Before we proceed to define our preconditioner and show spectral equivalence results, which imply uniform bounds on the condition number of the preconditioned system, we introduce some notation and summarize a few simple and well-known facts that are needed in the analysis (see, e.g., [9, 13]).

We denote by n the number of vertices in $\mathcal{T}_h$ and let $\{\varphi_i\}_{i=1}^n$ be the standard basis for $\mathcal{M}_h$. Since $\mathcal{V}_h = \mathcal{M}_h \oplus \mathcal{D}_h$, every $v \in \mathcal{V}_h$ can written as a sum of a continuous piecewise linear function in $\mathcal{M}_h$ and a discontinuous function in $\mathcal{D}_h$. Specifically, we have

$$v = v_c + v_d \in \mathcal{M}_h \oplus \mathcal{D}_h, \text{ where } v_c = \sum_{i=1}^n v_{c,i}\varphi_i(x), \quad v_d = \sum_{T\in\oplus_\langle} v_T(x-x_T)\mathbb{1}_T. \tag{5.12}$$

Here, $v_{c,i} = v_c(x_i) \in \mathbb{R}^d$, $v_T \in \mathbb{R}$, and $\mathbb{1}_T$ is the characteristic function of T. Note that $v_{c,i}$ are vectors, whereas the basis functions $\{\varphi_i(x)\}$ are scalar-valued functions.

With the above notation, we have the following matrix representation of the bilinear form $a(\cdot,\cdot)$:

$$\begin{aligned} a(v,w) = &\sum_{i,j=1}^n \boldsymbol{A}_{ij} v_{c,j}\cdot w_{c,i} + \sum_{i=1}^n \sum_{T\in\oplus_\langle} v_T \boldsymbol{A}_{T,i}\cdot w_{c,i} \\ &+ \sum_{T\in\oplus_\langle}\sum_{j=1}^n w_T \boldsymbol{A}_{j,T}\cdot v_{c,j} + \sum_{T\in\mathcal{T}_h}\sum_{T'\in\mathcal{T}_h} \boldsymbol{A}_{TT'} w_T v_{T'}, \end{aligned} \tag{5.13}$$

where $\boldsymbol{A}_{ij} \in \mathbb{R}^{d\times d}$, $\boldsymbol{A}_{T,i} \in \mathbb{R}^d$, $\boldsymbol{A}_{j,T} \in \mathbb{R}^d$, $\boldsymbol{A}_{T,T'} \in \mathbb{R}$ for $i = 1,\dots,n$, $j = 1,\dots,n$, $T \in \mathcal{T}_h$, $T' \in \mathcal{T}_h$, and their values are obtained using the definition of $a(\cdot,\cdot)$. Also, we

Copyright © by SIAM. Unauthorized reproduction of this article is prohibited.

Downloaded 05/04/22 to 144.174.212.73 . Redistribution subject to SIAM license or copyright; see https://epubs.siam.org/terms-privacy

denote by $\boldsymbol{A}$ the entire stiffness matrix of $a(\cdot,\cdot)$ of size $(dn+N_T)\times(dn+N_T)$, which is symmetric and positive definite (SPD). Note that the number of nonzero elements in each row of $\boldsymbol{A}$ is bounded by a constant due to the shape regularity of the mesh, and that constant will be denoted by $m_{\boldsymbol{A}}$. Now, let $v\in\mathcal{V}_h$ and $\mathbf{v}$ be the vector of degrees of freedom of v. Also, let $\boldsymbol{D}=\operatorname{diag}(\boldsymbol{A})$ be the diagonal of $\boldsymbol{A}$. Then, from the Cauchy–Schwarz inequality we can see that

$$[\boldsymbol{D}^{-1/2}\boldsymbol{A}\boldsymbol{D}^{-1/2}]_{lm}^2\le\frac{\boldsymbol{A}_{lm}^2}{\boldsymbol{A}_{ll}\boldsymbol{A}_{mm}}\le 1,\quad 1\le l,m\le(dn+N_T).$$

This in turn implies that $\left\|\boldsymbol{D}^{-1/2}\boldsymbol{A}\boldsymbol{D}^{-1/2}\right\|_\infty\le m_{\boldsymbol{A}}$, where $\|\cdot\|_\infty$ denotes the matrix infinity norm. Therefore,

$$\begin{aligned}\|v\|_{\mathcal{E}}^2=&\langle\boldsymbol{A}\boldsymbol{v},\boldsymbol{v}\rangle_{\ell^2}\le\rho\left(\boldsymbol{D}^{-1/2}\boldsymbol{A}\boldsymbol{D}^{-1/2}\right)\langle\boldsymbol{D}\boldsymbol{v},\boldsymbol{v}\rangle_{\ell^2}\\&\le\left\|\boldsymbol{D}^{-1/2}\boldsymbol{A}\boldsymbol{D}^{-1/2}\right\|_\infty\langle\boldsymbol{D}\boldsymbol{v},\boldsymbol{v}\rangle_{\ell^2}\le m_{\boldsymbol{A}}\langle\boldsymbol{D}\boldsymbol{v},\boldsymbol{v}\rangle_{\ell^2}.\end{aligned}\tag{5.14}$$

Here, $\rho(\cdot)$ denotes the spectral radius and $\langle\cdot,\cdot\rangle_{\ell^2}$ denotes the discrete ℓ^2-inner product.

Recall that any $v\in\mathcal{V}_h$ is multivalued at the vertices of the mesh because of the discontinuous nature of our EG space. For any $i\in\{1,\dots,n\}$, we let

$$v_{i,T}=v|_T(x_i)$$

for all $T\in\mathcal{T}_h$ containing the vertex x_i. We also define a jump of v at any vertex x_i on $e\in\mathcal{E}_h$ as follows:

$$[\![v]\!]_{i,e}=\begin{cases}v_{i,T_+}-v_{i,T_-} & \text{if } e\in\mathcal{E}_h^I \text{ and } e=T_+\cap T_-,\\ v_{i,T} & \text{if } e\in\mathcal{E}_h^\partial \text{ and } e\subset T.\end{cases}$$

Using the above notation, we will establish some equivalence relations.

Let K be a simplex in $\mathbb{R}^m$, $m\le d$, and v be a piecewise linear function. Then, we have

$$\|v\|_{0,K}^2\eqsim|K|\sum_{i\in K}|v_{i,K}|^2,\tag{5.15}$$

where $\sum_{i\in K}$ denotes the sum over all vertices x_i belonging to K. The constant in the equivalence depends on the dimension m of the simplex. A proof of this equivalence is available in many papers, for example, [15, Lemma 3.1]. Using (5.15), we then can write $a_J(\cdot,\cdot)$ in the following equivalent form:

$$a_J(v,w)\eqsim\widetilde{a}_J(v,w):=\sum_{e\in\mathcal{E}_h}\frac{\alpha_e|e|}{h_e}\sum_{i\in e}[\![v]\!]_{i,e}\,[\![w]\!]_{i,e}\,.\tag{5.16}$$

Last, we define two projection operators from $\mathcal{V}_h$ to $\mathcal{M}_h$, which will play a critical role in showing the spectral equivalence of $b(\cdot,\cdot)$ to $a(\cdot,\cdot)$. Let $\Pi_L:\mathcal{V}_h\to\mathcal{M}_h$ be the projection operator defined as

$$\Pi_L v=\sum_{i=1}^n\left[\frac{1}{m_i}\sum_{T\supset i}v_{i,T}\right]\varphi_i(x)\quad\forall v\in\mathcal{V}_h,\tag{5.17}$$

Copyright © by SIAM. Unauthorized reproduction of this article is prohibited.

Downloaded 05/04/22 to 144.174.212.73 . Redistribution subject to SIAM license or copyright; see https://epubs.siam.org/terms-privacy

where $m_i = \sum_{T \supset i} 1$ and $\sum_{T \supset i}$ denotes the sum over all elements T containing the vertex x_i, $i = 1, \ldots, n$. Let us assume that the domain $\cup_{T \supset i} T$ is a connected polyhedral domain for any $i \in \{1, \ldots, n\}$ and $T \in \mathcal{T}_h$. Then, for a fixed $i \in \{1, \ldots, n\}$ and $T \in \mathcal{T}_h$, the difference of the pointwise values of $v \in \mathcal{V}_h$ and $\Pi_L v \in \mathcal{M}_h$ at the vertex x_i can be estimated as follows:

$$\left| v_{i,T} - \frac{1}{m_i} \sum_{T' \supset i} v_{i,T'} \right|^2 \eqsim m_i \sum_{e \supset i} | [\![v_i]\!]_e |^2. \tag{5.18}$$

Such an equivalence relation follows immediately from the facts that the domain $\cup_{T \supset i} T$ is connected and that both left- and right-hand sides of (5.18) are then norms on the finite dimensional space $\mathbb{R}^{m_i}/\mathbb{R}$. The constants of equivalence depend on the shape regularity as m_i does depend on this as well.

We also introduce an elliptic projection $P_L : \mathcal{V}_h \to \mathcal{M}_h$ defined via a variational problem on $\mathcal{M}_h$:

$$a(P_L v, s) = a(v, s), \quad \forall v \in \mathcal{V}_h \ \forall s \in \mathcal{M}_h. \tag{5.19}$$

The following identities are obtained directly from the definition and the symmetry of $a(\cdot, \cdot)$:

$$a(P_L v, w) = a(w, P_L v) = a(P_L v, P_L w), \tag{5.20}$$

5.2.2. Additive Schwarz preconditioner. As previously stated, we will define our preconditioner by employing an additive Schwarz preconditioner. Here we point out that if we specify the action of an invertible preconditioning operator B, we then define its associated bilinear form $b(\cdot, \cdot)$ via (5.6), and vice versa. Let us now define the action of our preconditioner B on $g \in \mathcal{V}_h'$.

Algorithm 5.1 Additive Schwarz preconditioner for LF-EG.

function $w = B(g)$ ▷ Input: $g \in \mathcal{V}_h'$
  Find $v_L \in \mathcal{M}_h$ such that $a(v_L, \psi) = (g, \psi)$ for all $\psi \in \mathcal{M}_h$.
  Find $v_d \in \mathcal{V}_h$ such that $a_d(v_d, \chi) = (g, \chi)$ for all $\chi \in \mathcal{V}_h$.
  return $w = v_L + v_d$. ▷ Output: $Bg \in \mathcal{V}_h$
end function

Here, the bilinear form $a_d : \mathcal{V}_h \times \mathcal{V}_h \mapsto \mathbb{R}$ is yet to be specified. Roughly speaking, $a_d(\cdot, \cdot)$ will be chosen to satisfy that (a) it is SPD and (b) its induced norm is equivalent to a scaled $L^2(\Omega)$-norm. As we will see later in Lemma 5.6, these two requirements are sufficient to guarantee that $b(\cdot, \cdot) \eqsim a(\cdot, \cdot)$. A particular definition of $a_d(\cdot, \cdot)$ is given in (5.22).

Algorithm 5.1 is an instance of a two-level additive Schwarz preconditioner. The action of such a preconditioner requires the solution of two variational problems: one on $\mathcal{M}_h$ with $a(\cdot, \cdot)$ and the other on $\mathcal{V}_h$ with $a_d(\cdot, \cdot)$. We assume that optimal solvers are known for both of these forms. Indeed, on $\mathcal{M}_h$, the bilinear form $a(\cdot, \cdot)$ is spectrally equivalent to the vector Laplacian thanks to Korn's inequality, hence allowing for the use of standard multilevel solvers.

Let us now specify the bilinear form $a_d : \mathcal{V}_h \times \mathcal{V}_h \mapsto \mathbb{R}$ whose matrix representation is an approximate diagonal matrix of the stiffness matrix $\boldsymbol{A}$. The main role of the form $a_d(\cdot, \cdot)$ is to approximate $a(\cdot, \cdot)$ on the space complementary to $\mathcal{M}_h$ in $\mathcal{V}_h$. First,

Copyright © by SIAM. Unauthorized reproduction of this article is prohibited.

Downloaded 05/04/22 to 144.174.212.73 . Redistribution subject to SIAM license or copyright; see https://epubs.siam.org/terms-privacy

we will consider the diagonal of the stiffness matrix $\boldsymbol{A}$. With the notation introduced in (5.13), the diagonal of $\boldsymbol{A}$ consists of $\{[\boldsymbol{A}_{ii}]_{kk} | \, i = 1, \dots, n, k = 1, \dots, d \}$ and $\{\boldsymbol{A}_{TT} | \, T \in \mathcal{T}_h\}$. By recalling the definition of the bilinear form $a(\cdot, \cdot)$ in (5.2) and doing some straightforward calculations, we can estimate the diagonal elements as follows:

$$[\boldsymbol{A}_{ii}]_{kk} \eqsim \sum_{T \supset i} |T| \left(|\nabla \varphi_i|^2 + [\nabla \varphi_i]_k^2 \right) + \sum_{e \supset i; \, e \in \partial\Omega} \frac{\alpha_e}{h_e} \|\varphi_i\|_{0,e}^2 \eqsim \sum_{T \supset i} h_T^{-2} |T| (1 + \alpha_T),$$

$$\boldsymbol{A}_{TT} = d|T| + \sum_{e \in \partial T} \frac{\alpha_e}{h_e} \|x - x_T\|_{0,e}^2 \eqsim h_T^{-2} |T| \, (1 + \alpha_T) \sum_{i \in T} |x_i - x_T|^2,$$

where $\alpha_T = \frac{1}{d+1} \sum_{e \in \partial T} \alpha_e$ and we used (5.16) in the last equivalence. From these calculations, we see for any $v \in \mathcal{V}_h$ and its vector of degrees of freedom $\boldsymbol{v}$ that

$$\langle \boldsymbol{D}\boldsymbol{v}, \boldsymbol{v} \rangle_{\ell^2} \eqsim \sum_{T \in \mathcal{T}_h} h_T^{-2} |T| (1 + \alpha_T) \sum_{i \in T} v_{i,T}^2. \tag{5.21}$$

We are now ready to introduce $a_d : \mathcal{V}_h \times \mathcal{V}_h \mapsto \mathbb{R}$ and the corresponding operator $B_d^{-1} : \mathcal{V}_h \mapsto \mathcal{V}_h'$. For $v \in \mathcal{V}_h$ and $w \in \mathcal{V}_h$, we let

$$(B_d^{-1} v, w) = a_d(v, w) = \sum_{T \in \mathcal{T}_h} h_T^{-2} |T| (1 + \alpha_T) \sum_{i \in T} v_{i,T} w_{i,T}. \tag{5.22}$$

Then, the combination of (5.14), (5.21), (5.22) gives us that

$$a(v, v) = \langle \boldsymbol{A}\boldsymbol{v}, \boldsymbol{v} \rangle_{\ell^2} \leq m_{\boldsymbol{A}} \langle \boldsymbol{D}\boldsymbol{v}, \boldsymbol{v} \rangle_{\ell^2} \eqsim a_d(v, v). \tag{5.23}$$

Clearly, $a_d(\cdot, \cdot)$ is SPD and induces a norm $\|\cdot\|_{a_d}$ on $\mathcal{V}_h$. Also, $(P_L + B_d A)$ is invertible because B_d and A are both invertible and the positive semidefiniteness of P_L can be proved by taking $w = v$ in (5.20). Finally, we see that on a mesh with a characteristic size h, the form $a_d(\cdot, \cdot)$ is spectrally equivalent to a scaled $L^2(\Omega)$-norm. The matrix representation $\boldsymbol{B}$ of the preconditioner B can be expressed as

$$\boldsymbol{B} = \begin{bmatrix} \boldsymbol{I}_L \\ 0 \end{bmatrix} \boldsymbol{A}_L^{-1} \begin{bmatrix} \boldsymbol{I}_L & 0 \end{bmatrix} + \boldsymbol{B}_d, \tag{5.24}$$

where $\boldsymbol{A}_L$ is the stiffness matrix of $a(\cdot, \cdot)$ corresponding to the continuous linear elements, $\boldsymbol{B}_d$ is the matrix representation of B_d, and $\boldsymbol{I}_L$ is the $dn \times dn$ identity matrix.

5.2.3. Spectral equivalence and convergence. We begin this section with the following well-known result, which is found in many references (see [44, 46, 40, 45, 19] and the references therein) and is a main tool in showing the efficiency of the additive Schwarz preconditioner from Algorithm 5.1.

LEMMA 5.4. *The following relation holds for the preconditioner B defined via Algorithm* 5.1*:*

$$(B^{-1} v, v) = \inf_{w_L \in \mathcal{M}_h} \left(\|v - w_L\|_{a_d}^2 + \|w_L\|_{\mathcal{E}}^2 \right) \quad \forall v \in \mathcal{V}_h. \tag{5.25}$$

Proof. We set $(g, \cdot) = a(v, \cdot)$ for any $v \in \mathcal{V}_h$ in Algorithm 5.1 and consider the action of B onto it. From the definitions of the elliptic projection in (5.19) and of the

Copyright © by SIAM. Unauthorized reproduction of this article is prohibited.

Downloaded 05/04/22 to 144.174.212.73 . Redistribution subject to SIAM license or copyright; see https://epubs.siam.org/terms-privacy

bilinear form $a_d(\cdot,\cdot)$ in (5.22), we can see that $v_L = P_L v$ and $v_d = B_d A v$, hence we obtain $BAv = v_L + v_d = (P_L + B_d A)v$. Then, (5.7) yields

$$(B^{-1}v, v) = \left(A(BA)^{-1}v, v\right) = a\left((BA)^{-1}v, v\right) = a\left((P_L + B_d A)^{-1}v, v\right). \tag{5.26}$$

Let $q = B_d A(P_L + B_d A)^{-1}v$ and $q_L = P_L(P_L + B_d A)^{-1}v$. We note that $v = q + q_L$ with $q_L \in \mathcal{M}_h$ and $q \in \mathcal{V}_h$. Also, let $\widetilde{v} = (P_L + B_d A)^{-1}v$. Then, using (5.26), (5.22), and (5.20), we obtain that

$$\begin{aligned}(B^{-1}v, v) &= a\left((P_L + B_d A)^{-1}v, v\right) = a\left(\widetilde{v}, (P_L + B_d A)\widetilde{v}\right)\\ &= a\left(\widetilde{v}, B_d A\widetilde{v}\right) + a\left(\widetilde{v}, P_L\widetilde{v}\right)\\ &= a_d\left(B_d A\widetilde{v}, B_d A\widetilde{v}\right) + a\left(P_L\widetilde{v}, P_L\widetilde{v}\right) = \|q\|_{a_d}^2 + \|q_L\|_{\mathcal{E}}^2.\end{aligned} \tag{5.27}$$

On the other hand, for any $s \in \mathcal{M}_h$, we have

$$\begin{aligned}\|q - s\|_{a_d}^2 + \|q_L + s\|_{\mathcal{E}}^2 &= a_d(q - s, q - s) + a(q_L + s, q_L + s)\\ &= \|q\|_{a_d}^2 + \|q_L\|_{\mathcal{E}}^2 + \|s\|_{a_d}^2 + \|s\|_{\mathcal{E}}^2 - 2a_d(q, s) + 2a(q_L, s)\\ &= \|q\|_{a_d}^2 + \|q_L\|_{\mathcal{E}}^2 + \|s\|_{a_d}^2 + \|s\|_{\mathcal{E}}^2\\ &\quad -2a_d(B_d A(P_L + B_d A)^{-1}v, s) + 2a(P_L(B_d A + P_L)^{-1}v, s)\\ &= \|q\|_{a_d}^2 + \|q_L\|_{\mathcal{E}}^2 + \|s\|_{a_d}^2 + \|s\|_{\mathcal{E}}^2\\ &\quad -2a((P_L + B_d A)^{-1}v, s) + 2a((P_L + B_d A)^{-1}v, s)\\ &= \|q\|_{a_d}^2 + \|q_L\|_{\mathcal{E}}^2 + \|s\|_{a_d}^2 + \|s\|_{\mathcal{E}}^2\\ &\geq \|q\|_{a_d}^2 + \|q_L\|_{\mathcal{E}}^2.\end{aligned}$$

The equality holds in the above inequality if and only if $s = 0$. Therefore, we conclude that

$$\|q\|_{a_d}^2 + \|q_L\|_{\mathcal{E}}^2 = \inf_{s\in\mathcal{M}_h}\left(\|q - s\|_{a_d}^2 + \|q_L + s\|_{\mathcal{E}}^2\right) = \inf_{w_L\in\mathcal{M}_h}\left(\|v - w_L\|_{a_d}^2 + \|w_L\|_{\mathcal{E}}^2\right). \tag{5.28}$$

To see that the second equality in (5.28) holds, we set $w_L = (q_L + s) \in \mathcal{M}_h$ and observe that when s ranges over $\mathcal{M}_h$, so does w_L. Further, $(v - w_L) = (q - s)$ since $(q + q_L) = v$. We complete the proof by combining (5.27) and (5.28). ∎

We now prove the approximation and stability results.

LEMMA 5.5. *For any $v \in \mathcal{V}_h$, we have the estimates*

$$\|v - \Pi_L v\|_{a_d} \lesssim \|v\|_{\mathcal{E}}, \quad \|\Pi_L v\|_{\mathcal{E}} \lesssim \|v\|_{\mathcal{E}}, \tag{5.29}$$

where the constants of equivalence depend on the shape regularity of the mesh and the local variations in α_e.

Proof. Let $v \in \mathcal{V}_h$. To show the first inequality, we use (5.22), (5.17), and (5.18) to see

$$\begin{aligned}\|v - \Pi_L v\|_{a_d}^2 &\lesssim \sum_{T\in\mathcal{T}_h} \alpha_T h_T^{-2}|T| \sum_{i\in T}\left|v_{i,T} - \frac{1}{m_i}\sum_{T'\supset i} v_{i,T'}\right|^2\\ &\lesssim \sum_{T\in\mathcal{T}_h} \alpha_T h_T^{-2}|T| \sum_{i\in T}\sum_{e\supset i} |\,[\![v]\!]_{i,e}\,|^2.\end{aligned}$$

Copyright © by SIAM. Unauthorized reproduction of this article is prohibited.

Downloaded 05/04/22 to 144.174.212.73 . Redistribution subject to SIAM license or copyright; see https://epubs.siam.org/terms-privacy

Since we have $\frac{|T|}{h_T^2} \eqsim \frac{|e|}{h_e}$ by the shape regularity of the mesh, it follows that

$$\|v - \Pi_L v\|_{a_d}^2 \lesssim \sum_{T\in\mathcal{T}_h} \alpha_T \sum_{i\in T} \sum_{e\supset i} \frac{|e|}{h_e} |\llbracket v \rrbracket_{i,e}|^2 \lesssim \sum_{e\in\mathcal{T}_h} \alpha_e \sum_{i\in e} \frac{|e|}{h_e} |\llbracket v \rrbracket_{i,e}|^2.$$

Using now the relation (5.16), we arrive at

$$\|v - \Pi_L v\|_{a_d}^2 \lesssim \widetilde{a}_J(v,v) \lesssim \|v\|_{\mathcal{E}}^2. \tag{5.30}$$

To show the stability of Π_L, we employ the upper bound (5.23) to obtain

$$\|v - \Pi_L v\|_{\mathcal{E}}^2 \lesssim \|v - \Pi_L v\|_{a_d}^2,$$

which in combination with (5.30) gives rise to the desired result. ∎

We are now in a position to show the spectral equivalence between $a(\cdot,\cdot)$ and $b(\cdot,\cdot)$ using the stability results in Lemma 5.5.

LEMMA 5.6. *The following spectral equivalence holds:*

$$b(v,v) \eqsim a(v,v) \quad \forall v \in \mathcal{V}_h. \tag{5.31}$$

Proof. Let $v \in \mathcal{V}_h$. First, we will prove that $a(v,v) \lesssim b(v,v)$. To do this, take any $w_L \in \mathcal{M}_h$. By the triangle inequality, Young's inequality, and the upper bound in (5.23), we have

$$a(v,v) = \|v\|_{\mathcal{E}}^2 \le 2\left(\|v - w_L\|_{\mathcal{E}}^2 + \|w_L\|_{\mathcal{E}}^2\right) \lesssim \|v - w_L\|_{a_d}^2 + \|w_L\|_{\mathcal{E}}^2. \tag{5.32}$$

By taking the infimum with respect to $w_L \in \mathcal{M}_h$ on the right-hand side of (5.32), then using (5.25) in Lemma 5.4, we have

$$a(v,v) \lesssim (B^{-1}v, v) = b(v,v).$$

Next, the relation (5.25) in Lemma 5.4 and the estimates in (5.29) lead to

$$\begin{aligned} b(v,v) = (B^{-1}v, v) &= \inf_{w_L\in\mathcal{M}_h} \|v - w_L\|_{a_d}^2 + \|w_L\|_{\mathcal{E}}^2 \\ &\lesssim \|v - \Pi_L v\|_{a_d}^2 + \|\Pi_L v\|_{\mathcal{E}}^2 \lesssim \|v\|_{\mathcal{E}}^2 = a(v,v). \end{aligned}$$

The proof of the spectral equivalence is complete. ∎

THEOREM 5.7. *A preconditioned GMRES with the preconditioner B defined by Algorithm* 5.1 *is convergent uniformly with respect to the mesh size.*

Proof. Since we established that $b(\cdot,\cdot) \eqsim a(\cdot,\cdot)$ in Lemma 5.6, the field-of-values equivalence between B and S is an immediate consequence from Lemma 5.2. Then, the uniform convergence result follows from Theorem 5.3. ∎

6. Numerical examples in two dimensions. In this section, we present several numerical results in two dimensions to validate the theoretical results presented in sections 4 and 5 and demonstrate the efficiency and robustness of the proposed method. In our numerical experiments, the LF-EG and the preconditioned GMRES methods were implemented using the HAZmath finite element and solver library [24].

Example 1. Optimal convergence for a smooth solution. We test our proposed method on a smooth solution u to confirm the optimal convergence rate of

Copyright © by SIAM. Unauthorized reproduction of this article is prohibited.

Downloaded 05/04/22 to 144.174.212.73 . Redistribution subject to SIAM license or copyright; see https://epubs.siam.org/terms-privacy

the method proved in section 4. Our computational domain is $\Omega = (-1,1)^2$ and we choose the body force

$$f = [\ 2\sin(x)\sin(y), 2\cos(x)\cos(y)\ ]$$

so that the exact displacement is given by

$$u = \left[\ \sin x \sin y + \frac{1}{\lambda}x, \cos x \cos y + \frac{1}{\lambda}y\ \right].$$

We impose a Dirichlet boundary condition $u = u_D$, where u_D is computed from the exact solution. A simple calculation shows that $\nabla \cdot u \to 0$ as $\lambda \to \infty$, hence this solution is susceptible to volumetric locking for a large λ. In order to show the locking-free property along with the optimal convergence rate of our new method, we solve the elasticity problem with two different λ values ($\lambda = 1$ and $\lambda = 10^6$), while keeping $\mu = 1$, using our LF-EG method. Moreover, we solve the same problem with the classical linear CG method and compare the results to demonstrate the superiority of our new method over the CG method when simulating a nearly incompressible material.

Since the H^1-seminorm is bounded above by a constant multiple of the energy norm, we measure the error in the H^1-seminorm for both the LF-EG and P_1-CG methods on uniform meshes with various mesh sizes $h = 2^{-L}, L = 1, \ldots, 6$. For the LF-EG method, we set the penalty parameters to $(\alpha, \beta) = (1, 0.001)$, and the same parameters are used in all other numerical examples. The results are summarized in Table 1. In the tables, we observe that the linear CG method yields the optimal convergence rates in the H^1-seminorm when $\lambda = 1$, but its convergence rate deteriorates as h gets smaller when $\lambda = 10^6$. In contrast to this, the LF-EG method yields a first-order convergence in the H^1-seminorm for both $\lambda = 1$ and $\lambda = 10^6$. This example clearly demonstrates that the new LF-EG method can resolve the well-known

TABLE 1

Convergence study for the P_1-CG and LF-EG methods for Example 1 with (a) $\lambda = 1$ *and* (b) $\lambda = 10^6$. *The penalty parameters are set to* $(\alpha, \beta) = (1, 0.001)$.

	CG			LF-EG		
h	DoF	$\lvert u - U\rvert_1$	Rate	DoF	$\lvert u - U\rvert_1$	Rate
1/2	50	0.628	-	82	0.481	-
1/4	162	0.312	1.19	290	0.241	1.09
1/8	578	0.145	1.19	1090	0.120	1.05
1/16	2178	0.070	1.10	4226	0.059	1.02
1/32	8450	0.034	1.04	16642	0.029	1.01
1/64	33282	0.017	1.01	66050	0.014	1.00

(a) $\lambda = 1$.

	CG			LF-EG		
h	DoF	$\lvert u - U\rvert_1$	Rate	DoF	$\lvert u - U\rvert_1$	Rate
1/2	50	0.622	-	82	0.477	-
1/4	162	0.318	1.14	290	0.239	1.09
1/8	578	0.161	1.06	1090	0.119	1.04
1/16	2178	0.083	0.99	4226	0.059	1.02
1/32	8450	0.047	0.81	16642	0.029	1.01
1/64	33282	0.034	0.48	66050	0.014	1.00

(b) $\lambda = 10^6$.

Copyright © by SIAM. Unauthorized reproduction of this article is prohibited.

TABLE 2
Number of iterations for the preconditioned GMRES solver given in section 5 when the LF-EG method is applied to Example 1 with $\lambda = 1$ on meshes with various mesh sizes.

h	1/2	1/4	1/8	1/16	1/32	1/64
DoF	82	290	1090	4226	16642	66050
# of iterations	38	43	45	46	46	45

volumetric locking issue associated with the linear CG method by adding only one additional local DoF per element.

Example 2. Preconditioned GMRES solver. In this example, we test the performance of the GMRES method preconditioned as in section 5. The setup—exact solution, boundary conditions, and computational domain—is the same as that in Example 1. Since the theoretical results for the operator preconditioning show bounds on the condition number depending on the continuity of the bilinear form $\mathcal{S}(\cdot,\cdot)$, we use a fixed value of $\lambda = 1$. We test the LF-EG method on successively refined grids with mesh sizes $h = 2^{-L}$, $L = 1, \ldots, 6$. The iterations are terminated when the norm of the preconditioned relative residual is smaller than 10^{-9}. The results reported in Table 2 show that the number of GMRES iterations is independent of the mesh size as predicted by the theory studied in section 5.

Example 3. Alleviated volumetric locking. In a two-dimensional computational domain $\Omega = (0,1)^2$, we let the body force be $f = [0,0]$ and employ the following boundary condition:

$$u_D(x,y) = \begin{cases} [1-4(x-0.5)^2, 0] & \text{if } y = 0 \text{ or } y = 1, \\ [0,0], & \text{if } x = 0 \text{ or } x = 1. \end{cases}$$

This problem has been studied in other references [42, 43, 21] concerning volumetric locking. Here, we solve this problem with $\lambda = 1$ or $\lambda = 10^6$ using our LF-EG method and the P_1-CG method on a uniform mesh with a mesh size $h = 1/64$. The penalty parameters $(\alpha, \beta) = (1, 0.001)$ are used in the LF-EG method. Figure 2 provides the resulting solution profiles. We observe that the P_1-CG and LF-EG methods produce nearly identical solutions when $\lambda = 1$ (top). However, the two methods yield significantly different solutions when $\lambda = 10^6$ (bottom). In this case, we observe a visible locking phenomenon from the CG method.

Example 4. A solution with a corner singularity and a large λ. In this example, we consider the linear elasticity problem (1.1) in an L-shaped domain as depicted in Figure 3. This problem has a known analytic solution [2]. The exact solution is given in polar coordinates (r, θ) by

$$u_1 = \frac{1}{2\mu} r^\gamma \big((k - Q(\gamma+1))\cos(\gamma\theta) - \gamma\cos((\gamma-2)\theta)\big),$$
$$u_2 = \frac{1}{2\mu} r^\gamma \big((k + Q(\gamma+1))\sin(\gamma\theta) + \gamma\sin((\gamma-2)\theta)\big),$$

where $k = 3 - 4\nu$, $\nu = \lambda/(2(\lambda+\mu))$ is the Poisson ratio. In addition, γ is the solution of the equation

$$\sin\left(\gamma\frac{3\pi}{2}\right) + \gamma\sin\left(\frac{3\pi}{2}\right) = 0, \tag{6.1}$$

Copyright © by SIAM. Unauthorized reproduction of this article is prohibited.

Downloaded 05/04/22 to 144.174.212.73 . Redistribution subject to SIAM license or copyright; see https://epubs.siam.org/terms-privacy

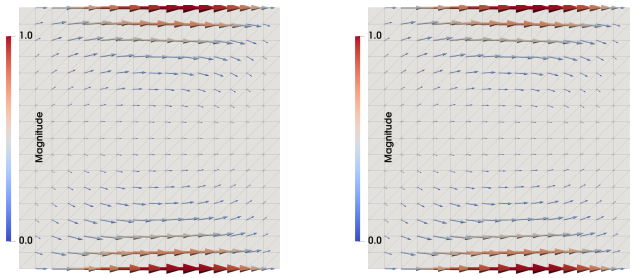

(a) P_1-CG ($\lambda = 1$). (b) LF-EG ($\lambda = 1$).

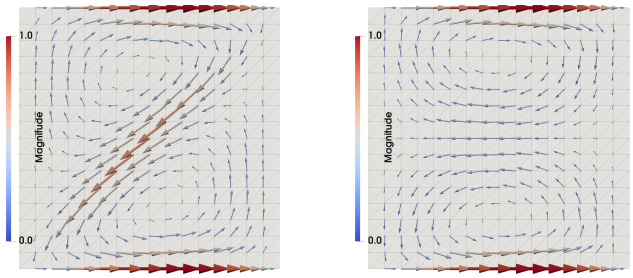

(c) P_1-CG ($\lambda = 10^6$). (d) LF-EG ($\lambda = 10^6$).

FIG. 2. *Comparison of the displacement profiles for Example* 3 *with* $\lambda = 1$ *(top) and* $\lambda = 10^6$ *(bottom) produced by* P_1*-CG and LF-EG methods.*

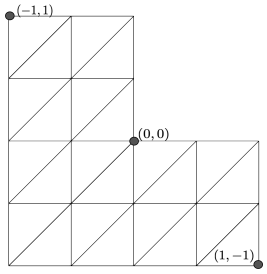

FIG. 3. *L-shaped domain.*

and Q is given by $Q = -\frac{\cos\left((\gamma-1)\frac{3\pi}{4}\right)}{\cos\left((\gamma+1)\frac{3\pi}{4}\right)}$. Then, the solution $u = [u_1, u_2]$ satisfies the linear elasticity equation (1.1) with the body force $f = [0, 0]$. Here, we set $\mu = 1$ and $\lambda = 10^6$ and employ the Dirichlet boundary condition. In our calculations, we numerically solve (6.1) to approximate γ, and the resulting values of γ and Q are $\gamma = 0.5444837367$ and $Q = 0.5430755688$. Since $\gamma < 1$, all the components for the stress tensor have a singularity in a neighborhood of the origin $(0, 0)$, while the displacement is continuous in the entire domain. Indeed, one can prove that $u \in H^{1+\gamma-\varepsilon}(\Omega)^2$ and $\sigma \in H^{\gamma-\varepsilon}(\Omega)^{2\times 2}$ for $\varepsilon > 0$ as discussed in [7]. Hence, we expect that the convergence rate of the new LF-EG method in the H^1-seminorm is approximately 0.54. This problem was solved using the LF-EG method with $(\alpha, \beta) = (1, 0.001)$ on uniform meshes. For the sake of comparison, we also solved the problem on the same meshes using the P_1-CG method. The results are summarized in Table 3. It is observed

Copyright © by SIAM. Unauthorized reproduction of this article is prohibited.

Downloaded 05/04/22 to 144.174.212.73 . Redistribution subject to SIAM license or copyright; see https://epubs.siam.org/terms-privacy

TABLE 3
Convergence study of the P_1-CG and LF-EG methods for Example 4.

	CG			LF-EG		
h	DoF	$\|u-U\|_1$	Rate	DoF	$\|u-U\|_1$	Rate
1/2	42	0.597	-	66	0.508	-
1/4	130	0.604	-0.02	226	0.350	0.61
1/8	450	0.660	-0.14	834	0.244	0.55
1/16	1666	0.703	-0.09	3202	0.167	0.57
1/32	6402	0.740	-0.07	12456	0.115	0.54
1/64	25090	0.770	-0.05	49666	0.078	0.56

that the P_1-CG locks in the sense that the errors measured in the H^1-seminorm stagnate. On the other hand, our new method converges at the expected rates in the H^1-seminorm.

7. Conclusions and future work. This paper introduced a new finite element method, called the LF-EG method, to address the well-known volumetric locking in the linear elasticity problem. The finite element space is obtained by adding only one additional local DoF per element to the linear CG space and used in the conventional DG formulation. An a priori error estimate in the energy norm was proved under the assumption of the H^2-regularity of the true solution. The resulting error estimate is of optimal order and independent of the Lamé constant λ, which implies the locking-free property of the method. Our numerical tests confirm the optimal convergence order for a smooth solution as well as the robustness of our LF-EG method with respect to the Lamé constant λ. They also show the expected suboptimal convergence order for a low regularity solution with a corner singularity. However, it remains open to prove the robust convergence without assuming the full H^2-regularity. Therefore, our method is a new alternative to other expensive numerical methods, including mixed finite element methods and DG methods, for simulating nearly incompressible materials. We also proposed a uniform preconditioner with respect to the mesh size in the framework of operator preconditioning for linear elasticity problems with a moderate-sized λ. We prove the uniform convergence of the preconditioned GMRES method and support our theoretical result through some numerical experiments. A theoretical and computational investigation on a uniform preconditioner for a large λ would require special treatment of the approximations of the divergence-free fields; hence it falls beyond the scope of this paper and is still an ongoing work.

REFERENCES

[1] R. A. ADAMS AND J. J. FOURNIER, *Sobolev Spaces*, Pure Appl. Math. 140, Elsevier, Amsterdam, 2003.
[2] M. AINSWORTH AND B. SENIOR, *Aspects of an adaptive hp-finite element method: Adaptive strategy, conforming approximation and efficient solvers*, in Symposium on Advances in Computational Mechanics, Vol. 2 (Austin, TX, 1997), Comput. Methods Appl. Mech. Engrg. 150, Elsevier, Amsterdam, 1997, pp. 65–87, https://doi.org/10.1016/S0045-7825(97)00101-1.
[3] T. ARBOGAST AND Z. TAO, *A direct mixed–enriched Galerkin method on quadrilaterals for two-phase Darcy flow*, Comput. Geosci., 23 (2019), pp. 1141–1160.
[4] D. ARNOLD AND G. AWANOU, *Rectangular mixed finite elements for elasticity*, Math. Models Methods Appl. Sci., 15 (2005), pp. 1417–1429.
[5] D. ARNOLD AND R. WINTHER, *Mixed finite elements for elasticity*, Numer. Math., 92 (2002), pp. 401–419.

Downloaded 05/04/22 to 144.174.212.73 . Redistribution subject to SIAM license or copyright; see https://epubs.siam.org/terms-privacy

Copyright © by SIAM. Unauthorized reproduction of this article is prohibited.

[6] D. N. Arnold, R. S. Falk, and R. Winther, *Mixed finite element methods for linear elasticity with weakly imposed symmetry*, Math. Comp., 76 (2007), pp. 1699–1723, https://doi.org/10.1090/S0025-5718-07-01998-9.
[7] I. Babuska and M. Suri, *The h-p version of the finite element method with quasi-uniform meshes*, RAIRO Modél. Math. Anal. Numér., 21 (1987), pp. 199–238.
[8] S. C. Brenner, *Korn's inequalities for piecewise H^1 vector fields*, Math. Comp., 73 (2004), pp. 1067–1087, https://doi.org/10.1090/S0025-5718-03-01579-5.
[9] S. C. Brenner and L. R. Scott, *The Mathematical Theory of Finite Element Methods*, 3rd ed., Texts in Appl. Math. 15, Springer, New York, 2008, https://doi.org/10.1007/978-0-387-75934-0.
[10] S. C. Brenner and L.-Y. Sung, *Linear finite element methods for planar linear elasticity*, Math. Comp., 59 (1992), pp. 321–338, https://doi.org/10.2307/2153060.
[11] N. Chaabane, V. Girault, B. Riviere, and T. Thompson, *A stable enriched Galerkin element for the Stokes problem*, Appl. Numer. Math., 132 (2018), pp. 1–21.
[12] J. Choo and S. Lee, *Enriched Galerkin finite elements for coupled poromechanics with local mass conservation*, Comput. Methods Appl. Mech. Engrg., 341 (2018), pp. 311–332.
[13] P. Ciarlet, *The Finite Element Method for Elliptic Problems*, Stud. Math. Appl., Elsevier, Amsterdam, 1978.
[14] D. A. Di Pietro and A. Ern, *A hybrid high-order locking-free method for linear elasticity on general meshes*, Comput. Methods Appl. Mech. Engrg., 283 (2015), pp. 1–21, https://doi.org/10.1016/j.cma.2014.09.009.
[15] V. A. Dobrev, R. D. Lazarov, P. S. Vassilevski, and L. T. Zikatanov, *Two-level preconditioning of discontinuous Galerkin approximations of second-order elliptic equations*, Numer. Linear Algebra Appl., 13 (2006), pp. 753–770, https://doi.org/10.1002/nla.504.
[16] R. S. Falk, *Nonconforming finite element methods for the equations of linear elasticity*, Math. Comp., 57 (1991), pp. 529–550, https://doi.org/10.2307/2938702.
[17] G. Fu, B. Cockburn, and H. Stolarski, *Analysis of an HDG method for linear elasticity*, Internat. J. Numer. Methods Engrg., 102 (2015), pp. 551–575, https://doi.org/10.1002/nme.4781.
[18] V. Girault, X. Lu, and M. F. Wheeler, *A posteriori error estimates for Biot system using enriched Galerkin for flow*, Comput. Methods Appl. Mech. Engrg., 369 (2020), 113185.
[19] M. Griebel and P. Oswald, *On the abstract theory of additive and multiplicative Schwarz algorithms*, Numer. Math., 70 (1995), pp. 163–180, https://doi.org/10.1007/s002110050115.
[20] P. Grisvard, *Singularities in Boundary Value Problems*, Recherches en Mathématiques Appliquées 22, Masson, Paris, 1992.
[21] P. Hansbo and M. G. Larson, *Discontinuous Galerkin methods for incompressible and nearly incompressible elasticity by Nitsche's method*, Comput. Methods Appl. Mech. Engrg., 191 (2002), pp. 1895–1908.
[22] G. Harper, R. Wang, J. Liu, S. Tavener, and R. Zhang, *A locking-free solver for linear elasticity on quadrilateral and hexahedral meshes based on enrichment of Lagrangian elements*, Comput. Math. Appl., 80 (2020), pp. 1578–1595, https://doi.org/10.1016/j.camwa.2020.07.014.
[23] M. Hauck, V. Aizinger, F. Frank, H. Hajduk, and A. Rupp, *Enriched Galerkin method for the shallow-water equations*, GEM Int. J. Geomath., 11 (2020), pp. 1–25.
[24] X. Hu, J. H. Adler, and L. T. Zikatanov, *HAZmath: A Simple Finite Element, Graph, and Solver Library*, https://bitbucket.org/XiaozheHu/hazmath/wiki/Home.
[25] T. Kadeethum, S. Lee, and H. Nick, *Finite element solvers for Biot's poroelasticity equations in porous media*, Math. Geosci., 52 (2020), pp. 977–1015.
[26] T. Kadeethum, H. Nick, S. Lee, and F. Ballarin, *Enriched Galerkin discretization for modeling poroelasticity and permeability alteration in heterogeneous porous media*, J. Comput. Phys., (2020), 110030.
[27] T. Kadeethum, H. Nick, S. Lee, and F. Ballarin, *Flow in porous media with low dimensional fractures by employing enriched Galerkin method*, Advances in Water Resources, 142 (2020), 103620.
[28] S. Lee, Y.-J. Lee, and M. F. Wheeler, *A locally conservative enriched Galerkin approximation and efficient solver for elliptic and parabolic problems*, SIAM J. Sci. Comput., 38 (2016), pp. A1404–A1429.
[29] S. Lee and M. F. Wheeler, *Adaptive enriched Galerkin methods for miscible displacement problems with entropy residual stabilization*, J. Comput. Phys., 331 (2017), pp. 19–37.
[30] S. Lee and M. F. Wheeler, *Enriched Galerkin methods for two-phase flow in porous media with capillary pressure*, J. Comput. Phys., 367 (2018), pp. 65–86.

Downloaded 05/04/22 to 144.174.212.73 . Redistribution subject to SIAM license or copyright; see https://epubs.siam.org/terms-privacy

Copyright © by SIAM. Unauthorized reproduction of this article is prohibited.

[31] D. Loghin and A. J. Wathen, *Analysis of preconditioners for saddle-point problems*, SIAM J. Sci. Comput., 25 (2004), pp. 2029–2049, https://doi.org/10.1137/S1064827502418203.
[32] K.-A. Mardal and R. Winther, *Preconditioning discretizations of systems of partial differential equations*, Numer. Linear Algebra Appl., 18 (2011), pp. 1–40, https://doi.org/10.1002/nla.716.
[33] P. Mital, *The Enriched Galerkin Method for Linear Elasticity and Phase Field Fracture Propagation*, Master's thesis, University of Texas at Austin, 2015.
[34] B. Rivière, S. Shaw, M. F. Wheeler, and J. R. Whiteman, *Discontinuous Galerkin finite element methods for linear elasticity and quasistatic linear viscoelasticity*, Numer. Math., 95 (2003), pp. 347–376, https://doi.org/10.1007/s002110200394.
[35] A. Rupp and S. Lee, *Continuous Galerkin and enriched Galerkin methods with arbitrary order discontinuous trial functions for the elliptic and parabolic problems with jump conditions*, J. Sci. Comput., 84 (2020), pp. 1–25.
[36] Y. Saad, *Iterative Methods for Sparse Linear Systems*, 2nd ed., SIAM, Philadelphia, 2003, https://doi.org/10.1137/1.9780898718003.
[37] Y. Saad and M. H. Schultz, *GMRES: A generalized minimal residual algorithm for solving nonsymmetric linear systems*, SIAM J. Sci. Stat. Comput., 7 (1986), pp. 856–869, https://doi.org/10.1137/0907058.
[38] S.-C. Soon, B. Cockburn, and H. K. Stolarski, *A hybridizable discontinuous Galerkin method for linear elasticity*, Internat. J. Numer. Methods Engrg., 80 (2009), pp. 1058–1092, https://doi.org/10.1002/nme.2646.
[39] S. Sun and J. Liu, *A locally conservative finite element method based on piecewise constant enrichment of the continuous Galerkin method*, SIAM J. Sci. Comput., 31 (2009), pp. 2528–2548.
[40] A. Toselli and O. Widlund, *Domain Decomposition Methods—Algorithms and Theory*, Springer Ser. Comput. Math. 34, Springer-Verlag, Berlin, 2005, https://doi.org/10.1007/b137868.
[41] M. Vogelius, *An analysis of the p-version of the finite element method for nearly incompressible materials. Uniformly valid, optimal error estimates*, Numer. Math., 41 (1983), pp. 39–53, https://doi.org/10.1007/BF01396304.
[42] T. P. Wihler, *Locking-free DGFEM for elasticity problems in polygons*, IMA J. Numer. Anal., 24 (2004), pp. 45–75, https://doi.org/10.1093/imanum/24.1.45.
[43] T. P. Wihler, *Locking-free adaptive discontinuous Galerkin FEM for linear elasticity problems*, Math. Comp., 75 (2006), pp. 1087–1102, https://doi.org/10.1090/S0025-5718-06-01815-1.
[44] J. Xu, *Iterative methods by space decomposition and subspace correction*, SIAM Rev., 34 (1992), pp. 581–613, https://doi.org/10.1137/1034116.
[45] J. Xu and L. Zikatanov, *The method of alternating projections and the method of subspace corrections in Hilbert space*, J. Amer. Math. Soc., 15 (2002), pp. 573–597, https://doi.org/10.1090/S0894-0347-02-00398-3.
[46] J. Xu and J. Zou, *Some nonoverlapping domain decomposition methods*, SIAM Rev., 40 (1998), pp. 857–914, https://doi.org/10.1137/S0036144596306800.
[47] S.-Y. Yi, *Nonconforming mixed finite element methods for linear elasticity using rectangular elements in two and three dimensions*, Calcolo, 42 (2005), pp. 115–133.
[48] S.-Y. Yi, *A new nonconforming mixed finite element method for linear elasticity*, Math. Models Methods Appl. Sci., 16 (2006), pp. 979–999.

Downloaded 05/04/22 to 144.174.212.73 . Redistribution subject to SIAM license or copyright; see https://epubs.siam.org/terms-privacy

Copyright © by SIAM. Unauthorized reproduction of this article is prohibited.